CRANFIELD UNIVERSITY

RICK HACKNEY

THE EFFECTS OF BLEED ON GAS TURBINE PERFORMANCE

SCHOOL OF AEROSPACE, TRANSPORT AND MANUFACTURING
Thermal Power

MSc (by research)
Academic Year: 2017–2018

Supervisor: Dr T. Nikolaidis
April 2018

CRANFIELD UNIVERSITY

SCHOOL OF AEROSPACE, TRANSPORT AND MANUFACTURING
Thermal Power

MSc (by research)

Academic Year: 2017–2018

RICK HACKNEY

The Effects of Bleed on Gas Turbine Performance

Supervisor: Dr T. Nikolaidis
April 2018

This thesis is submitted in partial fulfilment of the requirements for the degree of MSc (by research).

Abstract

The modelling of compressor interstage bleed in a gas turbine is required at all stages of the engine design cycle. The effect of the physical geometry of the bleed offtake on compressor flow is an important consideration, but of equal importance is the analysis of the effect of varying bleed amount and extraction stage on compressor work requirements and the overall gas turbine cycle. It is also important to obtain knowledge of the bleed air properties (temperature, pressure, work) for the purposes of secondary air systems downstream of the main gas path.

Current methods to identify these effects vary in terms of complexity and accuracy, and often require extensive manual adjustment of models. The aim of the project was therefore to investigate an innovative - yet simple - method of simulating any number of bleeds within a compressor without the need to compromise on model accuracy. Initially, a suitable modelling tool was identified. The Cranfield 0-D modelling software ”Turbomatch” has been validated against test data for a small industrial gas turbine, and it has been demonstrated that it can model engine performance within 0.5% to 1.0% accuracy for most parameters - well within the measurement uncertainty of the test data.

Subsequently, an alternate method has been proposed which offers a way simulating interstage bleeds through the implementation of two methods. Firstly, properties of the bleed air are calculated by utilising the polytropic relationship between pressure and temperature. Case studies performed on a number of Siemens industrial gas turbines suggest this is a valid method, with calculated stage pressure ratios within 3% of baseline studies, although older technology compressors tend to be modelled less accurately than newer ones. Secondly, compressor work requirements are calculated by use of the ”superposition principle” by implementing the work requirements of the bleed into a pre ’no bleed’ analysis calculation. This method has been implemented in the Cranfield modelling software Turbomatch, and validated against test data from an industrial gas turbine. Analysis so far show the method is quick, accurate, and compares within 1% of test data at all but the lowest off-design conditions.

Comparison of the alternative method against a compressor 'splitting' method showed comparable, and at off-design conditions, better, results can be obtained with the need for extensive manual model adjustment that the splitting method requires. This method has been implemented in 0-D cycle analysis software, which uses thermodynamic principles and component maps to calculate engine performance. Such a model tends to be used to analyse the overall effects of a component change on the engine cycle in a rapid and low-complexity manner (at a range of off-design conditions), whilst still producing a satisfactory level of accuracy. In the initial stages of a design project, the quick analysis and results from the 0-D software are essential to narrow down design choices and to analyse off-design performance. In this respect, the alternative method offers an enhancement to current methods for modelling bleed in the gas turbine.

Using this method to vary bleed stage and amount has been shown to change the engine running line and hence surge margin. This method can be used to produce three-dimensional plots showing the combined effect of beed amount and offtake stage location at a range of fixed parameters according to the user requirements (e.g. fixed speed, temperature or massflow).

Keywords

Compressor; Bleed; Modelling;Secondary Air System;Turbomatch

Contents

List of Figures

List of Tables

Nomenclature

Acronyms and Terminology

SGT	Siemens Gas Turbine (industrial engine)
CT	Compressor Turbine
PT	Power Turbine
SATM	School of Aerospace, Technology and Manufacturing
DCA	Double Circular Arc
MCA	Multiple Circular Arc
turndown air	Air that is bled from the exit of the compressor for emissions control

Symbols

C_p	Specific heat capacity
γ	ratio of specific heats
η	compressor efficiency
η_{th}	cycle thermal efficiency
$\dot{m}$	mass flow
UW	Useful work produced by free power turbine
$\dot{W}$	Work done between stations
$\dot{Q}$	Heat input
T	Total temperature
P	Total pressure
H	Total enthalpy
Δh	specific change in enthalpy between stations
ϕ	Bleed fraction at compressor stage
π	Stage pressure ratio
Π	Total pressure ratio
Z	Surge charecteristic, $(\Pi - \Pi_{choke})/(\Pi_{surge} - \Pi choke)$
N	Compressor speed
R	Universal gas constant

d	Diameter
ζ	Temperature per stage
δ	Stage pressure rise

Subscripts

Station numbering is based on ARP 755A[5]

2	Conditions at station 2 - Compressor inlet
21	Conditions at station 21 - Compressor bleed
3	Conditions at station 3 - Compressor exit
4	Conditions at station 4 - CT inlet
41	Conditions at station 41 - CT exit / PT inlet
5	Conditions at station 5 - PT exit
$fuel$	Conditions at fuel input into combustor
$isen$	isentropic
$poly$	polytropic
n	Compressor stage number, where n=specified stage
n_{last}	Total compressor stage count
$inlet$	Inlet parameter (used for dimensionless analysis)

Acknowledgements

The work described in this theis has been carried out at the School of Aerospace, Transport and Manufacturing of Cranfield University, where I conducted my industrial MSc research project under the supervision of Dr. Theoklis Nikolaidis. I would like to express my gratitude to you for you support, advice and patience.

I would like to give thanks to my colleagues at Siemens Industrial Turbomachinery for their support and understanding, and I would like to acknowledge the financial support from Siemens which has allowed me to undertake this project.

A special thanks to my parents and family for their undertanding and patience, and of course to my wife Carolyn for her support and encouragement throughout my studies - I could not have done it without you, and of course to Bailey for the good company and sound advice.

Chapter 1

Introduction

The development of a gas turbine, either by improving an existing design or by designing a new model is a costly but necessary process. Increasing thermal efficiency requirements and more stringent emissions legislation demand continuous improvement and development of gas turbine technology. Improvements to material technology, computational ability and general understanding allow such improvements to be made. However, all stages of the development cycle incur considerable costs. The gas turbine design procedure [1] , summarised in figure 1.1 , is a simplified overview of the design process showing the principal stages (note that in reality the process is rarely linear and numerous feedback and re-iterations of the design occur).

Those design stages where parts are manufactured and engines tested usually represent the most expensive stages of the design cycle. However, preliminary and conceptual design stages, whilst not typically as costly as the more physical parts of the cycle, are critical in that poor design at these stages can have huge cost implications further down the line. Thus having the correct tools and knowledge at all design stages to sufficiently model the gas turbine is crucial. Design tools come in a variety of forms, from relatively simple component mapping tools to full computational fluid dynamic analysis. The choice of tool depends on the stage of the project. At the early design phase, it is feasible that many design iterations may be investigated, a task which would take far too long using detailed modelling techniques.

1.1 Modelling

A model may be defined as *an abstract, mathematical, representation of a system* [2]. A good model provides an acceptable balance between accuracy and complexity for the system it represents. The definition of the system, however, can vary. For example, a model can represent the

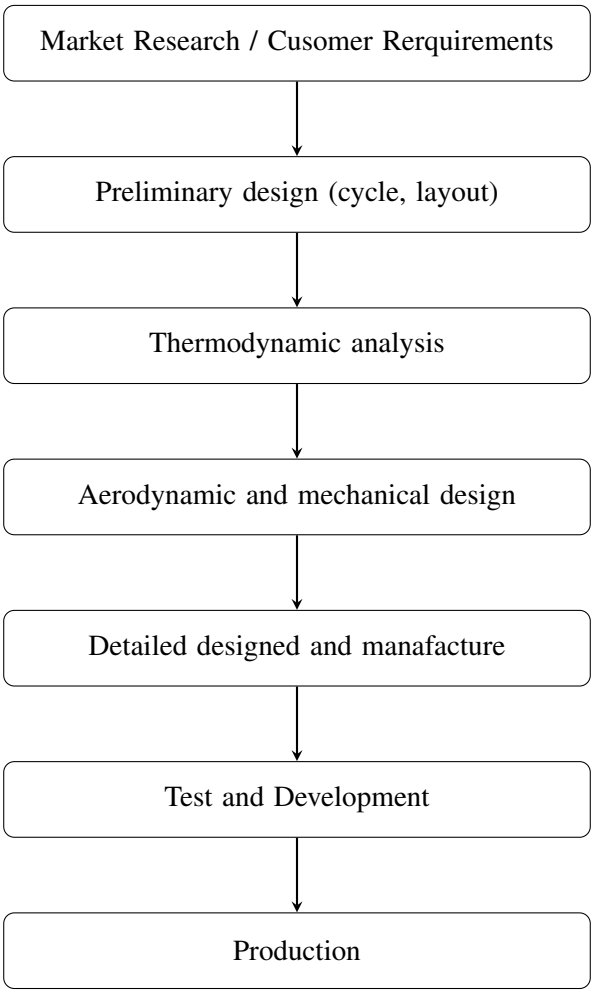

Figure 1.1: Gas Turbine Design Cycle. Adapted from [1]

entire gas turbine cycle, performing thermodynamic heat-balance methods to establish the overall performance of an engine, or it can represent individual components within the gas turbine (or even individual stages within that component). The method in which the model represents the system can be broadly divided into four categories in increasing order of detail and complexity, as demonstrated in table 1.1.

The level of detail provided by each category broadly increases from *0-D* to *3-D*. However, with this increase in *detail* there is an associated increase in complexity and time to to *set up* and *run* the models. There is no 'best' analysis standard - the choice of modelling method depends on the task in hand. In terms of the development process shown in figure 1.1, preliminary design and thermodynamic analysis stages tend to utilise 0-D or 1D modelling, where aerodynamic and mechanical design stages will utilise 2-D and even 3-D tools.

Model	Description	Examples
0-D	A series of reference points which relate system characteristics for a range of off-design points. No axial, radial or circumferential resolution [6]. Usually expressed non-dimensionally graphically or as a table	Compressor or turbine map
1-D	More detailed, physics based model including geometric characteristics. Flow assumed to be inviscid and one-dimensional [7]. Typically uses a mean radius along the axial length of a gas turbine component (meanline)	Compressor meanline analysis used to determine pressure and temperature for individual blade rows based on flow through the mean radius of the compressor
2-D	Inclusion of axial and radial flows within the component	Used in later stages of design process. For example, used to model secondary air system flows within a turbine
3-D	Full CFD analysis	Used where detailed analysis of flow structure is required for mechanical integrity

Table 1.1: Gas Turbine Design Tool Categorisation.

1.2 Efficiencies

It is important to understand that while the terms 'efficiency' and inefficiency' are used extensively in this report, the **efficiency of a component** has a different definition to the **thermal efficiency** of the gas turbine cycle. **Component efficiency** is measure of the energy change in the component compared to the *ideal* thermodynamic energy change (more on this later). Thus a value of unity (1.0) represents the thermodynamic ideal, while a (more typical) value of 0.90 represents 90% efficiency.

Thermal, overall, or cycle efficiency is simply a measure of the useful work produced by the gas turbine compared to the heat energy input to a system (e.g. output power divided by fuel energy input). The exact value varies considerably with many factors, but a simple-cycle efficiency (i.e. no waste heat recovery or combined cycle application) of 30-40% is not atypical.

1.3 Compressor

The compression cycle of the gas turbine (see section 2.1) is required in order to provide a working fluid to the turbine which is at a sufficiently high pressure ratio and temperature (through combustion) such that, once the work requirements of the compressor itself (and any other system losses) are met, there is a quantity of energy available to produce useful work to either a propelling nozzle or free power turbine.

The compressor is a crucial component within the gas turbine, and improvements to the efficiency of the compressor will yield a net benefit to the engine cycle through a reduction of work input required for the compressor, and thus result in an increased overall output power.

As with the design of any component, improvements to the efficiency can be gained by a reduction in the inefficiencies. Within the compressor, inefficiencies can be broadly categorised into three sources. Firstly, the **the non-perfect nature of the system** (i.e. heat or noise losses) will cause an increase in entropy and hence increase work requirements. Secondly, **leakage over the tips of compressor blades** will result in non-perfect compression of the working fluid, and finally, **the use of compressor air for secondary systems** within the engine or package/airframe. Clearly, then, being able to model the effect of component inefficiencies in the compressor on overall gas turbine thermal efficiency is necessary for modern engine design and development.

As the levels of development of gas turbine gas path components reaches higher and higher levels, the resulting further development margin is decreasing and has led to the consideration of factors not previously investigated in great deal [8]. Generally, improvements to gas turbines are seen through an increase in component efficiency, and it is the reduction of inefficiencies in these components that is the challenge. For example, a compressor of efficiency factor 0.90 must reduce inefficiencies by 10% in order to achieve an efficiency of 0.91. As this factor tends towards unity, the effort required to reduce component inefficiencies further becomes greater.

1.4 Compressor Bleed

Secondary air systems use some of the working fluid in the compressor to service other mechanical needs (such as turbine blade cooling or oil sealing) through the 'bleeding' of the main gas path air at selected axial locations along the compressor. The amount of bleed air can be as high as 30% of the total inlet massflow, so is clearly significant.

As shown in figure 1.2, Compressor bleed air can be defined as *a quantity of air which has been compressed at a specified stage of the gas turbine compressor for the use in secondary systems (such as cabin air systems, oil sealing or rotor thrust management).* Depending on its required use, this air may be reintroduced into the gas path of the turbine. As work has already been done to pressurise this air (the amount of which will depend on the stage at which the air is bled from, and the amount of air bled), bleed air represents an inefficiency in the overall gas turbine cycle. However, one study [9] suggested that any performance loss can be reduced or even inhibited if the bleed location is selected such that the matching of the compressor and turbine results in a greater pressure ratio than in the no bleed case. In either case, the need to model bleed accurately is clearly an important consideration

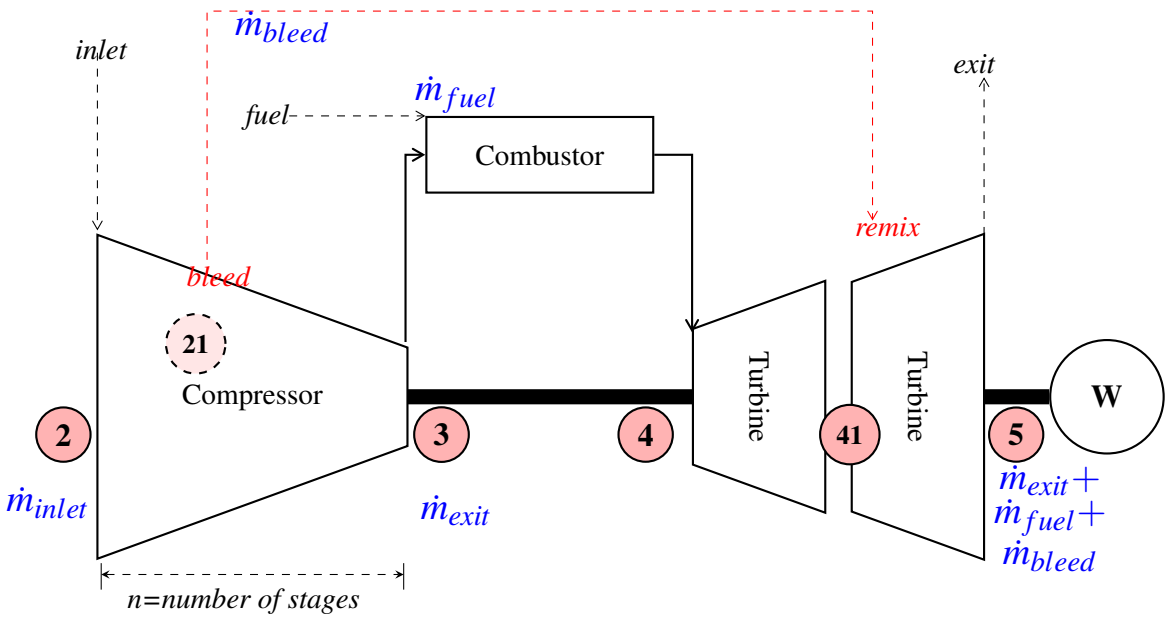

Schematic of secondary air systems on a single spool industrial free power turbine engine with interstage bleed remixing between free power turbine and compressor turbine. Numbers represent key stations for thermodynamic calculations. *2=compressor inlet, 21=compressor interstage bleed, 3=compressor exit, 4=compressor turbine inlet, 41=compressor turbine exit, 5=free power turbine exit. W* represents the driven unit

Figure 1.2: Engine schematic with bleed

1.5 Bleed modelling improvements

As bleed usually represents a source of inefficiency in a gas turbine system, it is important to account for this loss when modelling an engine cycle. As shown later in detail in section 5.2, as little as 2% air mass flow bleed can 'cost' an engine around 1% of useful work (which represents a 1% reduction in output power for a industrial gas turbine). When considering that design changes to gas turbines are often made to increase power by fractions of one percent, it is clearly important to model bleed correctly. The implementation of bleed may also affect the working line of the compressor, and hence change the surge margin.

The properties of the bleed air itself, specifically temperature and pressure, are also important considerations. For example, air bled at the wrong pressure may not flow into the main gas path at the required remixing location, or air used to cool components may be too hot to adequately cool

them and thus affect component lifing.

Consequently, nearly all modelling software will have the ability to model bleed. However, as discussed later in sections 2.5.4 and 2.5.5, there is a balance to be achieved between accuracy and complexity which is not always achieved. A method which offers both increased accuracy and relatively low complexity would therefore be a useful addition to a gas turbine model.

1.6 Project aims

A brief investigation into gas turbine design considerations has show that an investigation into methods which improve the modelling of an engine component is a suitable field of research for this thesis. This report analyses and discusses ways in which secondary air, or *compressor bleed* can be modelled and offers an alternative method to calculating the properties of bleed air and the effect on the overall gas turbine cycle. The aims of the project are thus:

1. For an axial compressor, derive a method which can be used to calculate bleed pressure and temperature without the need for complex modelling or detailed design knowledge
2. Derive a method which offers an alternative way to model the effect of bleed on the compressor and gas turbine cycle compared to current tools and methods (see section 2.5.5)
3. Investigate how bleed affects cycle efficiency and compressor surge margin

To achieve these aims, the following milestones were set:

- Develop an understanding of the main thermodynamic and aerodynamic principles which describe the gas turbine cycle
- Identify the main design considerations for compressor analysis and development
- Identify current methods for modelling the gas turbine, compressors, and compressor bleed
- Research current software and identify a suitable software package for integration of any alternative methods derived in this thesis

- Derive a method which offers an alternative way to model bleed and account for the effect of it in the gas turbine
- Integrate the method into analysis software
- Using test data, demonstrate the alternative method in action, and compare to the test data and other methods
- Discuss and demonstrate ways in which the alternative method can be used

1.7 Report structure

The literature review section (section 2.3.2) investigates the fundamental principles of gas turbine and compressor operation, and identifies ways in which bleed is modelled in the compressor. In order to understand the effect of compressor bleed on the engine, and to offer an alternative method of calculating these effects, the gas turbine cycle and principals of compressor operation are shown. An understanding of the various current modelling software is also discussed. This is shown in section 2.5.5.

Before any analysis is done, it is necessary to identify suitable modelling software to demonstrate the alternative method, and conduct a validation exercise against test data. This is shown in chapter 3

The derivation of the alternative method for modelling compressor bleed is shown in two sections. Chapter 4 shows how the properties of the bleed itself may be derived, and offers proof based on data from a number of Siemens industrial gas turbines. Chapter 5 shows a method for calculating the the effect of bleed on the gas turbine cycle and shows the demonstrates the use of this method using test data. Each of these chapters contain their own discussion section.

An analysis of the methods and results are discussed in chapter 6, and the effect of bleed on the compressor running line is also shown in this section. Finally, a conclusion and assessment of the project is made in the conclusion (section 7).

Chapter 2

Literature Review

2.1 Gas turbine Cycle

An understanding of the gas turbine cycle is required in order to perform any analysis of individual components within the engine. By plotting temperature (or enthalpy) against entropy (which is essentially a measure of heat energy which cannot be used for useful work, or a measure of inefficiencies within the system), the cycle can be analysed. Such a cycle is typically referred to as the Brayton, or Joule, cycle (where S=entropy and T=Temperature).

Shown in figure 2.1, the Brayton Cycle splits the gas turbine cycle into four main processes. Stage 1 to 2' represents isentropic compression of the working fluid (i.e. air) in the gas turbine from pressure P_{stage1} to pressure P_{stage2}. Associated with the increased pressure is a rise in temperature, and hence an increase of the energy of the air (i.e. increased enthalpy). This is followed by stage 2' to 3, which represents the addition of fuel to the working fluid, and combustion of the subsequent

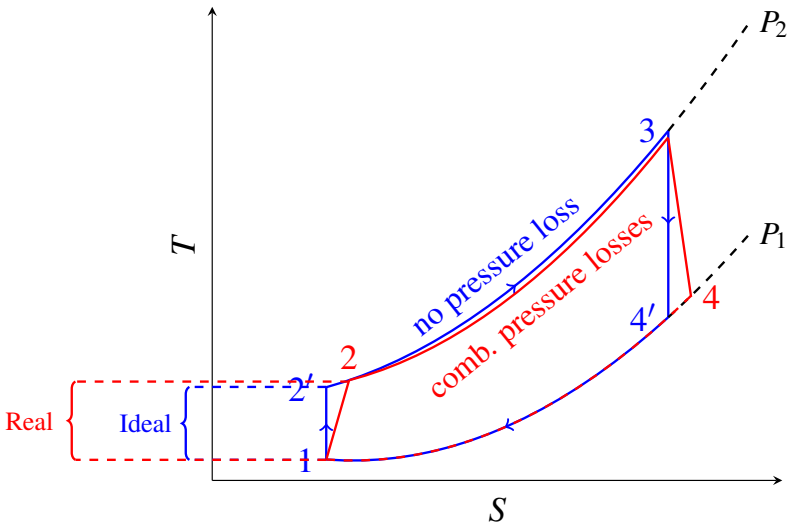

Figure 2.1: The Brayton Cycle

fuel-air mixture. This adds considerably more energy to the working fluid for the same pressure and hence increases temperature. Stage 3 to 4' represents isentropic expansion in the turbine where energy is extracted from the working fluid and is used to a) provide work to the compressor, and b) produce useful work output. Pressure is returned to P_{stage1} levels, and stage 4' to 1 represents the return to inlet conditions.

Graphically it can be seen that the difference between stage 1 to 2 is less than that of stage 3 to 4 (due to the addition of heat energy through fuel input). This implies that there is a greater temperature change during the expansion of the air compared to the compression. If the expansion process is responsible for providing energy to the compressor, then it can be assumed that $(\Delta T_{stage3-4} - \Delta T_{stage2-1}) \times C_p$ represents the remaining energy which can be used for useful work. By considering this change of energy per unit of mass flow, power can be calculated.

However, the cycle described above is the ideal cycle, which is defied by the following assumptions:

1. Compression and expansion is reversible and adiabatic (i.e. no heat or energy transfer between the system and its surroundings). A reversible and adiabatic system is known as an isentropic system
2. The change of kinetic energy between the inlet and outlet of each cycle is negligible.
3. There are no inlet, exhaust or combustion pressure losses (in reality, experience shows combustor losses are in the order of 4%).
4. The working fluid (i.e. air, or air and fuel), has the same composition throughout the whole process and is a perfect gas with constant specific heats (this essentially replaces combustion with heating).
5. Mass flow is constant.

To any observer, it is clear that the real gas turbine cycle is not ideal. The real cycle is also represented on figure 2.1 by *stages 1-2-3-4*, and differences are shown in table 2.1. This leads to the derivation of some fundamental thermodynamic expressions for work, heat and efficiency.

Stage in Cycle	Ideal Cycle Description	Real Cycle Description
1-2" (ideal), 1-2 (real)	Isentropic compression	Actual compression
2"-3 (ideal), 2-3 (real)	Combustion at constant pressure	Combustion with pressure losses
3-4" (ideal), 3-4 (real)	Ideal turbine work	Real turbine work
4"-1 (ideal), 4- 1 (real)	Heat rejection at constant pressure	Heat rejection with pressure loss

Table 2.1: Ideal vs real operation as represented in the Brayton Cycle (figure 2.1)

.

As discussed earlier, total heat energy, or *total enthalpy* is found from the following:

$$H = C_p T \tag{2.1}$$

Where H=Total Enthalpy, C_P=Specific heat at constant pressure, and T=Total temperature. Power absorbed, or work produced ($\dot{W}$) is therefore the change in enthalpy per unit massflow, $\dot{m}$

$$\dot{W} = \dot{m} C_p \Delta T \tag{2.2}$$

This is a fundamental equation as it can be used to show how much power a component (i.e. turbine) produces, or how much work a component (i.e. compressor) requires. Knowledge of the work requirements of the compressor is critical if the effect of bleed on work is to be analysed.

The equation which satisfies the first law of thermodynamics for the Brayton cycle is the steady flow energy equation. For the gas turbine, this is expressed as:

$$\begin{aligned} Q - W &= \Delta H \\ Q - W &= \dot{m} C_p \Delta T \end{aligned} \tag{2.3}$$

Where Q=power (heat) input and W=power output. This equation clearly shows that the useful work from a gas turbine is equal to the energy put in minus the cycle work requirements. By changing the cycle work requirements (through bleed, for example), the amount of useful work will be changed.

So, for each stage represented in the Brayton cycle:

$$\begin{aligned} W_{12} &= -(h_{stage2} - h_{stage1}) = -C_p(T_{stage2} - T_{stage1}) \\ Q_{stage2-3} &= (h_{stage3} - h_{stage2}) = C_p(T_{stage3} - T_{stage2}) \\ W_{stage3-4} &= (h_{stage3} - h_{stage4}) = C_p(T_{stage3} - T_{stage4}) \end{aligned} \tag{2.4}$$

For a simple cycle (i.e. no waste heat recovery through the exhaust gasses), cycle thermal efficiency is simply the ratio of net work output to heat supplied through the addition of fuel (which is determined by the amount of fuel flow and calorific value of the fuel). Expressed in terms of equation 2.4 this becomes:

$$\eta_{th} = \frac{C_p(T_{stage3} - T_{stage4}) - C_p(T_{stage2} - T_{stage1})}{C_p(T_{stage3} - T_{stage2})} \tag{2.5}$$

Where η_{th} = cycle thermal efficiency. Similar to equation 2.3, this equation shows how the thermal efficiency of the gas turbine may be derived using the energy in, work requirements, and output power.

A fundamental expression is the isentropic relationship between pressure and temperature:

$$\left(\frac{T_{stage2}}{T_{stage1}}\right) = \left(\frac{P_{stage2}}{P_{stage1}}\right)^{\left(\frac{\gamma-1}{\gamma}\right)} \tag{2.6}$$

Where T_{stage2} and T_{stage1} represent compressor exit and inlet temperature respectively, P_{stage2} and P_{stage1} are the equivalent pressures at the same stations, and γ is the ratio of C_p and C_v (specific heat at constant pressure and specific heat at constant volume). P_{stage2}/P_{stage1} is referred to as the *pressure ratio* and is shortened to Π. Knowledge of this relationship can be used to calculate the efficiency of a component or, if the efficiency is known, the temperature/pressure ratio. This is used later to show how bleed pressure can be calculated.

2.2 Normalisation of data

It is clear from the Brayton cycle that the temperature and pressure at the start of the cycle (point 1) will have a significant influence on the overall cycle power and thermal efficiency. Therefore it is desirable to account for this variability by normalising the data to conditions such that analysis may be done on a 'like for like' basis. Normalisation of data is usually done in one of three ways.

Dimensionless groups contain all variables affecting engine performance, such as temperature, pressure and fluid properties, as well as linear scaling factors [10], and are the most accurate form of non-dimensional analysis.

Quasidimensionless groups tend to omit many of the air properties, such as the specific gas constant and gamma. This method is relevant for most analysis of components in the gas turbine. While strictly speaking the air properties should be accounted for, this method is suitable for assessing the operational conditions of a component or engine. While this group is sometimes referred to as *non-dimensional*, many of the quasidimensionless expressions do in fact have units (although this does not affect the validity of the analysis).

Corrected groups are directly proportional to quasidimensionless groups but differ in that, rather than expressing data as semi-dimensionless, the results are *corrected* to a given set of conditions. The advantage of corrected data over quasidimensionless data is that it offers a tangible understanding of the data. For example, it may be hard to grasp the significance of a a quasidimensionless massflow of 280 , but the equivalent corrected massflow of $40 kg/s$ has much more meaning. For these reasons corrected results are often used for commercial purposes or test analysis.

When using corrected data, it is important to state what the given set of conditions are. For industrial gas turbines, the International Standards Organisation (ISO) standard *BS EN ISO2314* [11] defines the industry standard corrected conditions. These conditions tend to be termed *ISO conditions* (as they are referred to within this document), and are shown in table 2.2. Also included in table 2.2 are other fundamental assumptions made when normalising engine data. While strictly speaking inlet and exhaust duct pressure drops do not have a normalisation expression, it is important to remove the effect of ducting pressure loss from corrected data. This is because the

arrangement of ducting varies considerably from site to site, and even between test berths. For aero engines, the International Standard Atmosphere (ISA) defines standard day ambient temperature and pressure up to an altitude of 30 500m [10], and conditions at sea level are the same as ISO conditions.

A comparison of the three groups of normalised data for temperature, pressure, speed and massflow is shown in table 2.3. Of particular interest are the quasidimensionless expressions for pressure, speed and massflow, as these represent the main parameters on the *compressor map* (see section 2.3.1).

2.3 Compressor

2.3.1 Compressor Map

The primary purpose of the compressor is to increase the total pressure of the gas stream whilst absorbing the minimum shaft power as possible [10]. The axial compressor comprises of a number of stages, each one comprising of a rotor and a stator. In its most basic terms, the rotor accelerates the working fluid which is decelerated in the stator in the stator blade passages, converting kinetic energy to static pressure. This is repeated for each stage of the compressor until the desired pressure ratio (the ratio of pressure at compressor outlet to that at the inlet) is obtained [1]. Figure 2.2 shows a schematic of an axial flow compressor. As the compressor comprises of a number of stages, each with an associated temperature and pressure rise, it is important to know which stage air is bled from. Note that the annulus of the compressor changes axially in order to keep the axial

Inlet Parameter	**Value**
Inlet air temperature	288.15K
Inlet air pressure	1.013bar
Relative Humidity	60%
Inlet duct losses	none
Exhaust duct losses	none
Gearbox efficiency	100%

Table 2.2: ISO zero-loss conditions

Parameter	**Dimensionless**	**Quasidimensionless**	**Corrected (ISO)**
Temperature at station n	$\frac{C_p\,(T_n/T_{inlet}-1)}{\gamma R}$	$\frac{T_n}{T_{inlet}}$	$\frac{T_n}{\theta}$
Pressure at station n	$\frac{C_p\left(\left(P_n/P_{inlet}\right)^{\frac{\gamma-1}{\gamma}}-1\right)}{\gamma R}$	$\frac{P_n}{P_{inlet}}$	$\frac{P_n}{\delta}$
Speed ($d = diameter$)	$\frac{N\times d}{\sqrt{\gamma\times R\times T_{inlet}}}$	$\frac{N}{\sqrt{T_{inlet}}}$	$\frac{N}{\sqrt{\theta}}$
Massflow, W ($d = diameter$)	$\frac{W\sqrt{T_{inlet}\times R}}{d^2\times R\times P_{inlet}}$	$\frac{W\times\sqrt{T_{inlet}}}{P_{inlet}}$	$\frac{W\times\sqrt{\theta}}{\delta}$
Corrrection Factors			
Temperature, θ	$\frac{T_n}{288.15}$	Pressure, δ	$\frac{P_n}{1.0135}$

Table 2.3: Comparison of normalised expressions

velocity constant - this is just one of many design considerations which need to be made.

The characteristics of a typical axial compressor may be expressed graphically as a non-dimensional map. Figure 2.3 shows a typical compressor map for an industrial gas turbine. Pressure ratio (essentially non-dimensional) is plotted against the non-dimensional flow, and lines of constant non-dimensional speed are drawn. The non-dimensional compressor isentropic efficiency is also plotted as lines of constant non-dimensional speed. There are a number of key characteristics shown on this plot which are important to consider:

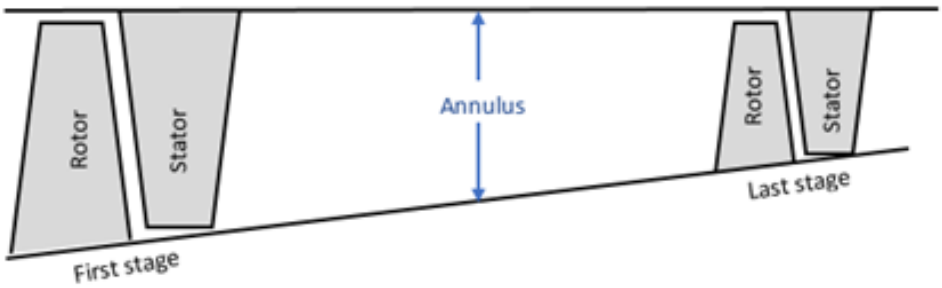

Figure 2.2: Axial Flow Compressor

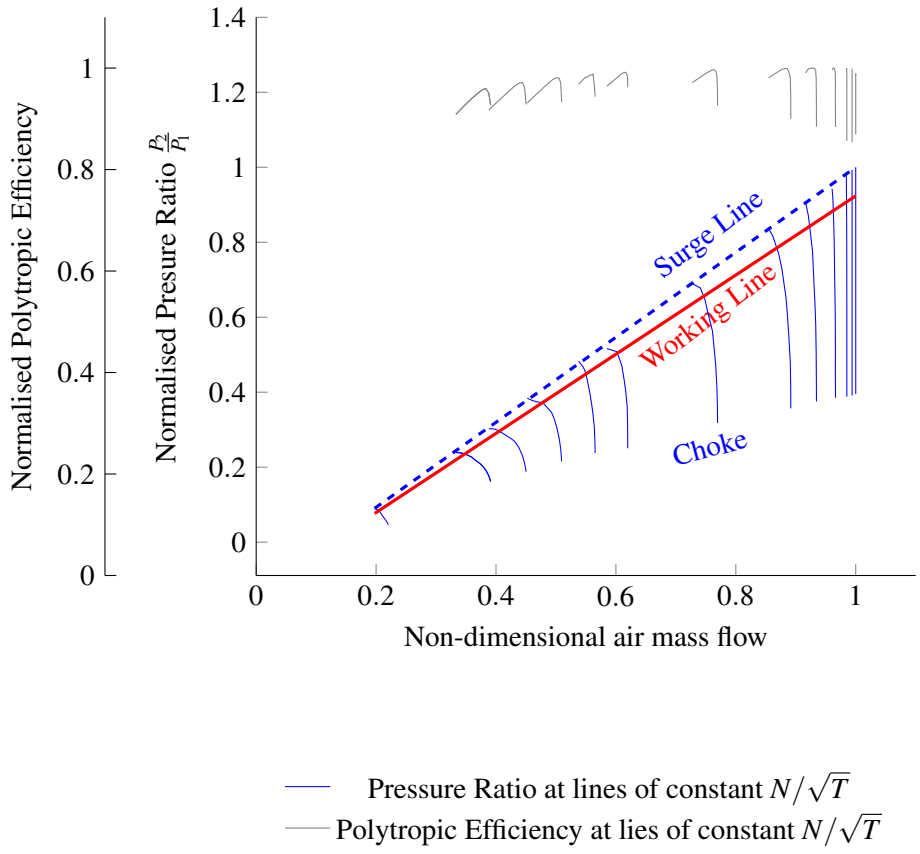

Figure 2.3: Compressor Map

Non-dimensional analysis

All parameters are shown non-dimensionally, which means that they are independent of ambient temperatures and pressures, and thus engines operating at different ambient conditions can be represented by the same map.

Speed Lines

As speed increases the lines of constant speed bunch together and become more vertical. This is because the front stage blades are becoming choked (the point at which the mass flow has reached its maximum value, regardless of how much pressure ratio is reduced)

Efficiency Lines

Similar to the speed lines, these represent lines of constant isentropic efficiency. The running line of the engine tends to be based on peak efficiency for each non-dimensional speed line.

Surge Line

Surge occurs when blade stall (usually a result of excessive relative angle between flow direction

and blades) become so excessive that the adverse pressure gradient can no longer be maintained [1]. This causes a rapid reversal in flow direction which, if no rectification action is taken, will then result in flow re-establishing and another surge. The surge would continue at a rate between 5 to 10Hz [10], eventually resulting in damage to the engine. The surge line represents the upper limit of the normal running window.

Running Line

The running line (or working line) is normally set at the maximum value of isentropic efficiency for a given speed. The margin between the running line and surge line is known as the surge margin.

It can be seen from figure 2.3 that the difference between the surge line and working line - the surge 'margin' - is smaller at low non-dimensional speeds. This is a typical characteristic of a modern compressor, and care must be taken that at these low speeds (i.e. during start) there is enough margin such that the compressor does not reach conditions which will cause surge. While surge at low speeds is much less damaging to the engine than a high speed surge, it may well prevent an engine from starting.

It is therefore unsurprising that the surge margin is a crucial consideration in compressor design. For that reason, gas turbine designers control the flow of the compressor where margins are tight using mechanical means, such as variable blade geometry and interstage bleed.

The use of *variable blade geometry* has the effect of raising the surge line by changing the flow angle of the compressor stage and thus reducing flow at a speed. This moves the surge line to the left of standard. *Interstage bleed* valves do not affect the compressor map, but instead move the running line of the engine downwards (assuming a single stage compressor, not multi-spool). While bleed valves have a higher impact on the efficiency of the engine (compressed air is essentially being dumped to the atmosphere rather than going through the engine), they are cheaper and more reliable than variable blade geometry [10]. Quite often both methods are employed in an engine. The Siemens range of SGT engines, for example, all use both variable blade geometry and interstage bleed to control low speed surge margin.

2.3.2 Compressor Design Considerations

Section 2.3.1 shows how the operating characteristics of the compressor may be expressed as a non-dimensional map, and how this map can be used to identify the running line (i.e. maximum efficiency line), surge line, and choke region. This is vital information to an engineer designing a compressor to ensure that it will function correctly in the design operating range of the gas turbine. However, there are a number of other secondary design considerations which should be identified. Using figure 2.4, which is a representation of the compressor as a black box (i.e. for the purposes of this discussion it does not matter if it is a 0-D or 1-D model), it is possible to summarise the most significant primary and secondary compressor design considerations [10]. $N/\sqrt{T}$ refers to non-dimensional compressor speed while β refers to lines of constant turbine operating temperature - both of which are used to define the "running line" of the compressor.

Note that bleed is shown as one of three 'secondary' outputs from the model (the primary outputs being flow, pressure and temperature of the main gas path).

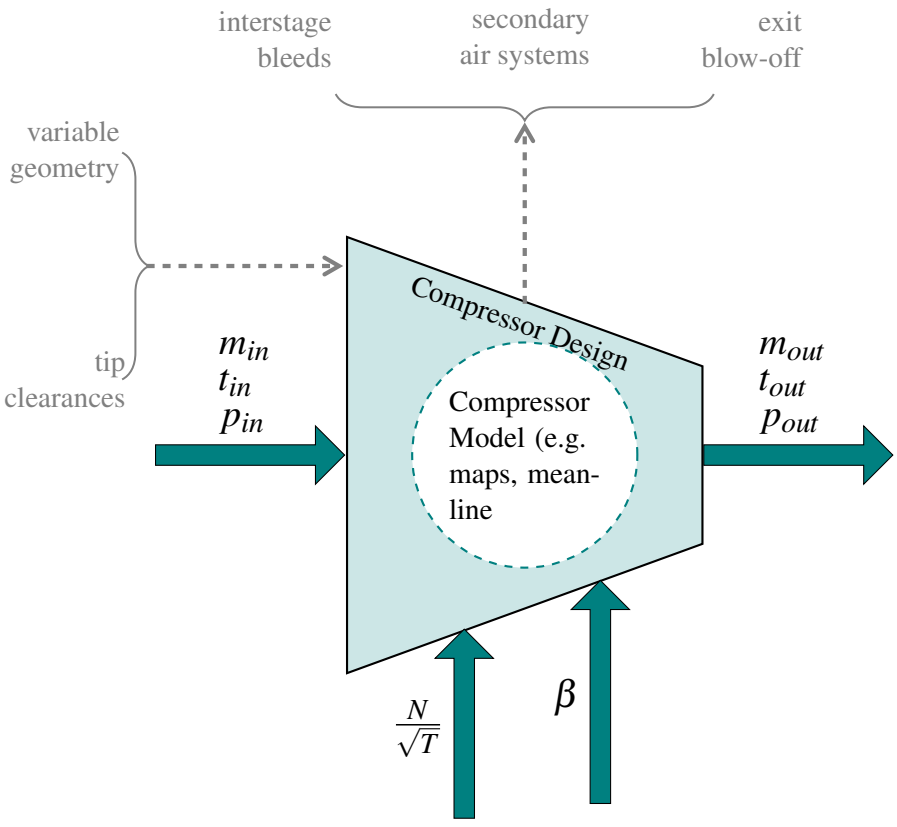

Figure 2.4: Compressor design considerations (adapted from [2]).

Compressor speed

The maximum speed should be specified such that the mechanical integrity of the compressor is not adversely affected by the rotational speed. Care must also be taken to ensure that the engine does not frequently run at the same harmonic speeds of the compressor blades ('critical speeds'), and that excursions through these 'criticals' are as quick as possible.

Blade clearances

Rotor to stator blade clearances (and vice-versa) must be carefully monitored to ensure that they are not excessively large and thus reduce the overall efficiency of the compressor, which in turn leads to higher work requirements for the compressor and a reduction on overall engine efficiency, or too small that they are at risk of cutting into the casing due to thermal expansion and possibly causing damage to the blades.

Tip clearance is the radial gap between rotor blades and the outer casing. Larger or smaller tip clearances effectively represent a change in compressor geometry and hence change the compressor map [10]. On smaller gas turbines, where clearances represent a more significant proportion of overall blade height, excessive tip clearances can have a significant effect on stage efficiency. Not only is efficiency lost, but surge margin is reduced. This can be a particular problem on overhauled engines where blade components may be dressed and re-used. In these cases, care must be taken to ensure the blades are to original specifications, else the risk of surge is increased.

Air flow properties

Care must be taken to ensure that the axial velocity of the flow is within design margins. For example, the design of the blades will vary considerably depending whether the flow is subsonic, transsonic or supersonic.

Variable Geometry

Already discussed in section 2.3.1, variable geometry is an important consideration not just for surge margin management at low speeds, but also for speed management of the engine at other load conditions. The Siemens SGT-400 small industrial gas turbine has a variable geometry modulation region at high loads in order to control compressor speed. This means the engine can operate at higher loads without reaching speed limitations. In the case of single-spool engines (where speed is fixed due to the driven unit requirements), variable geometry modulation will change the air

mass flow into the engine and as such may be used for part load emissions control.

Compressor air offtake for stability and emissions control

Already discussed in section 2.3.1, interstage bleed may be used to move the working line of the compressor and hence increase surge margin. It can also be used to control emissions on an engine by diverting a proportion of the compressor exit air downstream of the turbine. Known as *turndown air*, this has the effect of raising the operating temperature of the engine for a given power, although there is a slight reduction in overall thermal efficiency (equation 2.5). This higher operating temperate allows low CO emissions to be maintained at relatively low loads. Note that at these conditions, while the operating temperature is higher than a no-turndown case, it is still sufficiently low that thermal NOx formation is small.

Secondary air bleed The secondary air system is critical for the safe operation of the engine. Table 2.4 summarises the main uses of secondary air systems, as described by Foley (2001) [12].

The amount of air used as secondary air varies from engine to engine and is a closely guarded secret by manufacturers of gas turbines. However, typically 10 to 30% of the main core flow is allocated to secondary air [12]. The majority of this air is allocated to blade cooling. This is especially true of more modern engines, where increases to the Turbine Entry Temperature require increasing amounts of cooling air in order to maintain acceptable blade metal temperatures. Clearly, then, the design of secondary air systems is an important part of the design of a modern gas turbine.

However, the design of secondary air systems is complex. Nearly all components within the

Category	Examples
Cooling	Turbine rotor blades, turbine nozzles, rotor discs, combustion cans, engine casings
Sealing	Disc cavities, bearings, shafts
Ventilation	Bearing chambers, rotor cavities
Bearing thrust modification	Used to tune' thrst bearing loads
Aircraft services	Cabin pressurisation, cabin heating, anti-iciing

Table 2.4: Examples of secondary air systems

gas turbine have some impact on the secondary air system, and the plethora of passages, seals, drilling and cavities mean that calculations of air flows and effectiveness are best suited to the more advanced modelling tools, which due to complexity and considerable processing requirements are not best suited for the early stages of gas turbine design. These tools also tend to concentrate on properties of the air downstream of the compressor and its effect on downstream components. In many modelling tools the effect of bleeding air from the compressor on the compressor itself is not often considered in any detail, and consequently the effect of design changes which result in different bleed requirements may not be properly modelled in the engine.

Optimisation of secondary air should systems also be considered. When designing a new compressor, air can be designed to be bled from the compressor at almost any stage along its axis. Bleed requirements may well be fixed (e.g. sealing air must be at a certain pressure), and thus offer no flexibility in location or amount of bleed, but in some circumstances there may well be some flexibility. For example, the requirements for bleed air that is used for heating, such as cabin air, will be based on the heat energy of the bleed air. Heat energy is defined as $\dot{W} = \dot{m}C_p\Delta T$, and thus it can be observed that the massflow/temperature relationship may be varied and still result in the same output heat energy. In these circumstances an optimisation exercise, where the location and amount of bleed is selected to give the minimal compressor work requirements while still providing the same heat energy, may be performed.

2.3.3 Compressor Blade Design

The design of compressor blades has evolved much over the past 50 years, and has had a significant effect on efficiency and stage pressure ratio. In general, the trend is towards greater pressure ratio for less stages of axial compressor. Table 2.5 shows the advances in the Siemens range of industrial gas turbines. It can be seen that as blade technology level increases, the move is away from C4 style-blades and onto DCA or MCA variations, depending on the relative velocity. As all three blade variations are still in use today (certainly within industrial engines), the analysis of a method to calculate bleed properties should consider a range of blade technology levels.

In early axial compressors, the flow over the rotor blade was entirely subsonic (i.e. lower than the speed of sound). Air flow relative to the blade is typically expressed as a Mach number (the ratio

Engine	Date	Blade Technology Level	Power (MW)	Pressure Ratio	Stages	PR/Stage
TB5000	1970	C4	3.9	7.8	12	0.7
SGT-200-1S	1981	C4	6.75	12.3	15	0.8
SGT-100-1S	1989	DCA	4.7	14.1	10	1.4
SGT-300-1S	1995	MCA	7.7	13.9	10	1.4
SGT-400 13MW	2000	DCA	12.9	16.9	11	1.5

Table 2.5: Changing pressure ratio with increasing technology level for selected Siemens industrial gas turbines. Adapted from [1]

of the air velocity relative to the speed of sound for the same air). Blade design typically followed the NACA-65 or C series. Early Siemens engines were designed using the C series, which tend to have a blunter leading edge than other blade designs, leading to a more robust blade, but one that is less suited to high Mach number operation (as the flow turning capabilities of this blade design are poor at high Mach numbers). Maximum thickness tends to be at 30% of chord [3]. The camber of the blade tends to describe either a circular of parabolic arc.

However, to achieve higher pressure ratio per stage, it was necessary to increase flow across the blades to near-transonic or transonic speeds (typically defined as a flow velocity just above and below supersonic - around Mach 0.7-1.2). The double circular arc (DCA) blade was designed for such uses, and has maximum thickness at around 50% of chord width [3]. This tends to produce a more sharp nose compared to the blunter C4 design, and has a large effect on the velocity distribution. This effectively resulted in a higher pressure ratio compressor for a lower number of stages, as well as higher efficiency. Figure 2.5 shows the typical profile difference between ”C4” and ”DCA” style blades. More modern engines further refined blade design and utilised Multiple Circular Arc (MCA) blades, which were capable of even higher relative velocities and thus a further improvement in pressure ratio and efficiency.

As a general guide, Wright [13] suggests that C4 type designs are suitable for Mach numbers less than 0.78, but between 0.7 and 1.2 Mach number the DCA design is more suited. As Mach number increases above 1.1, non-negligible shock losses as well as secondary losses resulting shock separation from the boundary layer become significant [13] and the multiple circular arc (MCA) blade series are more suitable. Frost *et al* [14] states that the MCA blade design incorporates and

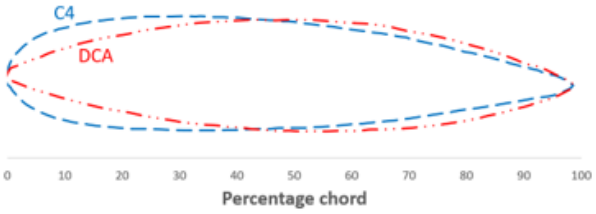

Figure 2.5: C4 vs DCA blade profile. Adapted from [3]

extends the circular-arc definition to include the potential for defining a camber line composed of two segments, either or both of which may be either circular arcs or straight lines. The application of straight sections in the blade camber reduces losses associated with parts of the blade which have supersonic flow.

2.4 Efficiency

It has already been established that the real gas turbine cycle is not ideal, and losses exist due to an increase in entropy. If it is assumed that the overall cycle efficiency is the ratio of actual to ideal work, the following expression is observed:

$$\eta = \frac{W'}{W} = \frac{\Delta H'}{\Delta H} \tag{2.7}$$

Where η=compressor efficiency and suffix ' represents actual cycle operation (see Brayton cycle in figure 2.6). Substituting equation 2.2 into equation 2.7 gives the following (note C_p is effectively cancelled out):

$$\eta_c = \frac{T'_{stage2} - T_{stage1}}{T_{stage2} - T_{stage1}} \tag{2.8}$$

This is also shown on figure 2.6 as the difference between real and ideal compressor temperature rise.

Finally, by substituting the isentropic expression (equation 2.6) in terms of T_1 into equation 2.8 and rearranging, an expression for the isentropic efficiency (η_{isen}) of the compressor can be obtained:

$$\eta_{isen} = T_{stage1}\left[\frac{(\Pi_{comp})^{\frac{\gamma-1}{\gamma}} - 1}{T_{stage2} - T_{stage1}}\right] \tag{2.9}$$

Where Π_{comp} = compressor pressure ratio. A similar calculation may be derived for the turbine using the same principles described in this chapter. Knowledge of the isentropic efficiency means that, for a given temperature rise, the pressure rise (or pressure ratio) may be calculated. This is equally true in reverse (temperature may be calculated from a known pressure rise). Being able to perform this calculation is a key part of the alternative method to calculate individual compressor stage properties described within this report, although as explained below, isentropic efficiency is not necessarily the best method to use.

2.4.1 Isentropic and Polytropic Efficiency

By considering the temperature rise of the compressor on a stage-by-stage basis, one can see a fundamental characteristic of the isentropic efficiency. Figure 2.6 shows a magnification of the Brayton cycle during the compression stage. By plotting individual stage isentropic temperature rise on a fictional 5-stage axial compressor (ΔT_{s1} to ΔT_{s5}), it can be seen that the sum of the individual stage isentropic temperature rise is greater than the whole temperature rise, $\Delta T_{2'-1}$. This implies that the work input in the latter stages to produce a specified pressure rise is greater than that in the earlier stages. Thus the isentropic efficiency of latter stages is lower than that of earlier stages, which is somewhat misleading, and implies that the more stages of a compressor, the lower the efficiency of that compressor. Thus it is clear that the *overall* isentropic efficiency would not represent all stages of the compressor adequately.

This can be avoided by incorporating another definition of efficiency —the polytropic efficiency. By effectively using ΔT_{2-1} as the temperature rise assumption, Cumsty [3], suggests that for all processes $Tds = dh - dp/p$ and that for an adiabatic and reversible one $dh_s = dp/p$. For real compression, the enthalpy rise dh will be larger than the isentropic rise dh_s and thus:

$$dh = \frac{1}{\eta_{poly}} dh_s = \frac{1}{\eta_{poly}} \frac{dp}{P} \tag{2.10}$$

If η_{poly} is assumed constant over a finite change on pressure, then for a perfect gas:

$$\left(\frac{T_{stage2}}{T_{stage1}}\right) = \left(\frac{P_{stage2}}{P_{stage1}}\right)^{\left(\frac{\gamma-1}{\gamma\eta_{poly}}\right)} \tag{2.11}$$

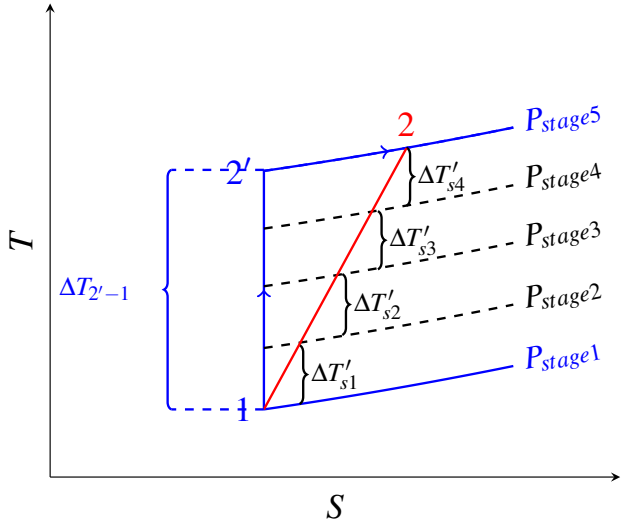

Figure 2.6: The Brayton Cycle, showing difference between polytropic and isentropic definitions

Re-arranging gives:

$$\eta_{poly} = \frac{\ln\left(\frac{P_{stage2}}{P_{stage1}}\right)^{\left(\frac{\gamma-1}{\gamma}\right)}}{\ln\left(\frac{T_{stage2}}{T_{stage1}}\right)} \tag{2.12}$$

The difference between polytropic and isentropic efficiency for different pressure ratios can be seen in figure 2.7. It can be seen that for a constant value of polytopic efficiency, isentropic efficiency varies across the entire pressure ratio range (although for very low pressure ratios - less than 1.5 - the difference between isentropic and polytropic is less than 0.5%. This may partly be attributed to low pressure ratios typically having a relatively consistent isentropic efficiency between stages). In an axial compressor, it can therefore be assumed that isentropic efficiency varies per blade stage. Due to the this variability over the axial length of the compressor it is preferable to use the *polytropic* efficiency when comparing overall compressor performance. This is because it removes the penalty for higher pressure ratios so that compressors of similar design, yet different pressure ratios, may be compared without the higher pressure ratio penalty of using isentropic efficiency.

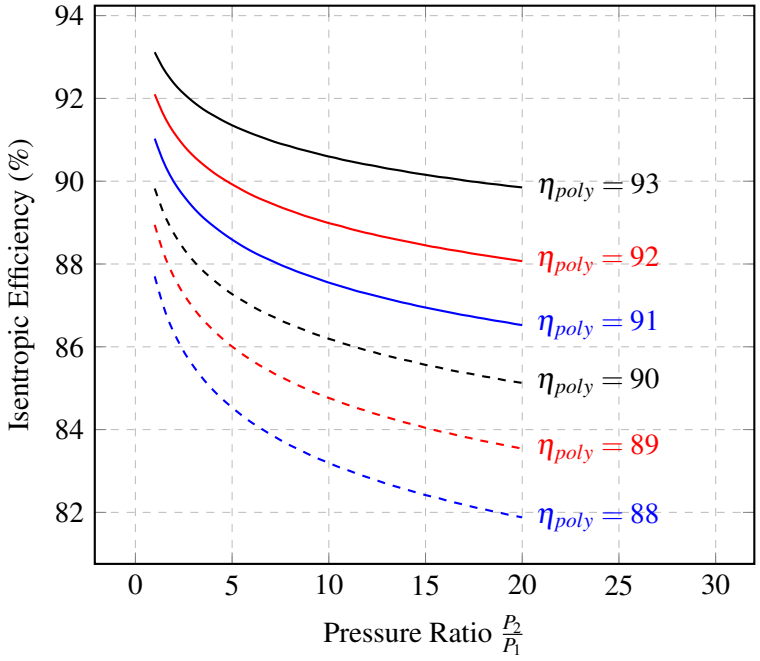

Figure 2.7: Isentropic vs. Polytropic efficiency over varying pressure ratio

2.5 Modelling

The method in which the gas turbine (and hence compressor bleed) is modelled will depend on the complexity level, stage of the development cycle and type of software used, as discussed in the following sections.

2.5.1 Design concept software

At the very early design concept stage, design concept software may be used to optimise gas turbine component design. For example, Siemens Industrial Turbomachinery in Lincoln uses in-house software GT-Design, which is a performance prediction conceptual design program for complete gas turbine cycles. Comprising of three primary modules (1-D compressor, combustor and 1-D turbine), GT-Design performs design-point calculations for new and phantom engine studies. The relatively simplistic nature of this software means that it is well-suited to initial design-point concepts, but it lacks complexity (especially in the compressor module) and is not suited for off-design performance calculations.

Jeschke et al (2002) [15] suggest that a modern prototype preliminary design program must meet the following requirements:

- Assessment of all major engine components and their interrelations
- Inclusion of relevant disciplines
- Design over several operating points
- Model fidelity zooming capabilities for individual components

The modelling of bleed within design concept software would either be done as part of the 1-D meanline compressor analysis, or incorporated into the overall gas tubine cycle by adjustments to the compressor air flows. These methods are further discussed in the next section as part of the analysis of other modelling tools.

2.5.2 Off-design modelling

If the design point (DP) represents the component characteristics at the optimum condition (the optimum condition being specified according to the running requirements of the engine, and is usually at the maximum efficiency point of a component), then *off-design* (OD) conditions represent areas away from this optimum condition. While the design point is clearly a primary consideration in the development of a gas turbine, it is equally important to ensure that the engine meets requirements at off-design conditions. An aero engine, for example, may well have a design point based on a nominal cruise setting, but off-design performance for purposes such as take-off, taxi and climb must also be considered. For an industrial engine with a free power turbine driving a compressor, a large amount of the engines running regime may be conducted at off-design conditions.

So, while design point performance is usually the 'first step' in analysing the performance of an enigne, it is essential that modelling software exists which can calculate off-design performance. Some types of software are more suitable to this task than others, as discussed in the following section.

2.5.3 Types of models

Ordered in approximate order of increasing detail and complexity, the following section describes typical gas turbine modelling tools.

Map-based iterative modelling

Beyond the initial design concept change, an engine may be modelled by considering the engine as as series of (experimentally and theoretically derived) non-dimensional component maps, and reference design point thermodynamic parameters. It is then possible to perform an iterative calculation to predict gas turbine performance at a range of conditions. This is achieved through the use of a software package, and most gas turbine manufacturers and academic institutions will have some form of proprietary software.

Map based solutions offer a highly flexible approach to modelling a gas turbine, and can quickly produce a working model at a range of design and off-design conditions. While the level of detail may not be as much as some of the other tools discussed below, they do tend to consider the entire gas turbine cycle and can even accommodate ancillary systems. Gas turbine cycle definition and analysis is one of the most important activities during the preliminary design phase, and aids in determining the component specification, engine configuration, and gives preliminary performance estimates over a wide range of operating conditions (both design point and off-design point).

Such tools are not only used during preliminary design phases of projects. Due to their nature - the prediction of performance over a wide range of operating conditions - they are also utilised as sales tools, and can perform engine health monitoring by a comparison of actual performance to model performance.

Component Zooming

Representing a slightly more resource intense method, *compressor zooming*, which is defined as using *...a higher order component analysis code ...[to] ...adjust the zero-dimensional component performance characteristics within the [0-D] system simulation"*[7], may be utilised as it

offers a balance between level of detail and resource requirements. However, such a method still requires a considerable level of knowledge of the compressor. Essentially this method takes the relative simplicity of the map-based analysis and only adds complexity where required. However, depending on the complexity of the 'zoomed' component, this may limit off-design point analysis.

The process of zooming is used by Bolemant and Peitsch (2014) [2] to create a hybrid map and meanline method. The map is used for first order effects and meanline analysis used for secondary effects (such as variable geometry changes). The effects of the secondary effects are then applied as deltas to the map. For example, bleed offtakes in the compressor induce changes in the flow field due to swirl and temperature distribution [2], which in turn will affect the compressor map and stage efficiency. Such analysis cannot be easily included in normal compressor-map based design, and suggests that hybrid analysis techniques such as zooming are required to investigate effect in more detail.

Stage Stacking

Stage stacking is a method of modelling the compressor as a series of sequential stage characteristic curves. These curves are usually represented by relationships between flow coefficient, pressure coefficient and efficiency [16]. By performing a stage by stage calculation, where the output from the previous stage acts as the input to the current stage, a calculation of compressor performance is obtained. While this method is relatively straightforward and simple, it is a more complex calculation that an overall map based analysis. The user must also provide detailed information on each stage's characteristics which is less likely to be known at early design stages. It is also not particularly useful as part of a whole engine matching exercise, due to the relative complexity of the method. For this reason, stage stacking tends to be used for analysis of the component in isolation. However, Song *et al.* (2001) [16] have developed a method where each stage is solved simultaneously by solving the governing equations of the system using the Newton-Rhapson method. While this method demonstrated a greater flexibility in selecting boundary conditions, and allowed for the modelling of bleed at any stage in the compressor, it nevertheless is still a relatively complex method compared to an overall map based method.

Mean line analysis

Mean line analysis ignores any radial variation in airflow and gas properties and considers axial variation only. In some respects this makes it similar to the stage stacking method, as stage stacking is essentially an axial analysis of component performance. However, where stage stacking uses component maps to describe competent properties, mean line analysis uses the fundamental thermodynamic and airflow equations to determine performance. Mean line analysis has been demonstrated by Veres (2009) [17] to be a suitable method for off-design analysis of a axial compressor. This method is best applied to design conept work, as it is able to produce an estimation of the sizing and other physical properties of the (concept) compressor. While capable of performing off-design analysis, the user would need to understand the various stage properties and component dimensions in order to perform the analysis.

Computational-Fluid Dynamics (CFD)

At the most detailed level, a full CFD simulation of air flows, compressor geometry and bleed offtake geometry may be conducted [18]. While such a method may yield detailed results, the time taken to produce the results and the detailed knowledge required of the components(s) to be modelled mean that such an exercise is too resource intense for initial analysis. Similarly, analysis of off-design performance requires another full iteration of the CFD analysis.

2.5.4 Modelling bleed as part of map based analysis

As discussed in section 2.5.3, map based solutions are a suitable tool for modelling a gas turbine and associated systems at all stages of the design process, and are especially useful at the early design stage or during off-design analysis. The handling of bleed, however, may be done in a number of ways.

All bleed at compressor exit uses the assumption of all bleed is at compressor exit. The user simply assumes that all interstage bleed occurs the compressor exit, prior to combustion. No assumptions of bleed temperature and pressure are required, but conversely this means that these

values will be highly inaccurate when downstream remixing is introduced (this may or may not be an issue depending on what the bleed air is used for). While this method does ensure that the bleed air is not part of the main gas path into the combustor, it makes no assumption of the change in work requirements for the compressor.

Linear compressor assumptions may be used to obtain an estimate of temperature and pressure for each stage assuming that each stage has an equal temperature and pressure rise (the accuracy of which is discussed later in this report). While this method may yield better estimations for pressure and temperature than assuming all bleed is at compressor exit, it still does not specifically account for the change in compressor work due to the massflow of bleed at a specific stage (although this may be done in conjunction with other methods such as splitting of the compressor, shown below).

Splitting of the compressor 'splits' the compressor into a number of sub compressors using a previous compressor model and dividing into a number of sections determined by the interstage bleed locations. Providing the user has calculated the design point inlet and outlet conditions of each sub compressor correctly, this method may result in a high level of accuracy as the bleed is essentially modelled in the correct axial location. Bleed temperatures and pressures may also be more representative depending on the method used to calculate them. This method is demonstrated in more detail in later sections.

2.5.5 Current modelling Software

Chapter 1 discusses the importance of having a suitable modelling tool for each of the phases in the design process. All manufacturers and developers of a gas turbine will utilise a map-based cycle analysis tool of some form. These may be commercially available products or in-house proprietary packages. Some examples are discussed below.

Proprietary Industrial Models

Siemens Industrial Turbomachinery, based in Lincoln, use the in-house performance prediction tool 'MATCH' for the analysis of steady state design point (DP) and off-design (OD) performance analysis. It is designed to be used for both single spool (e.g. power generation) and free-power

turbine configurations of engines. The tool itself is split into a number of modules/subroutines, each of which represent a step in the overall algorithm (e.g subroutine to read in the compressor map, subroutine to calculate the turbine inlet conditions) [19].

Data for a specific engine model is provided through three primary inputs. Firstly, a series of *O-D* non-dimensional component maps describe the characteristics of the primary components (compressor, combustor, turbine, exhaust diffuser). Secondly, an engine data file is specified which contains mechanical and build characteristics of the engine (e.g. bleeds, heat losses, mechanical losses, remixes). Finally, a data file is created by the user which contains the operating conditions to be modelled (such as ambient conditions, inlet and exhaust pressure drops, compressor and turbine speed, operating temperature).

Steady state performance is calculated by following the mass and energy conservation laws, and iterations take place using a modified Newton-Raphson [20] method until an engine 'match' is found. The software also has the option to scale the maps in order to better 'match' the model to a particular engine or design scenario.

Secondary air systems are stated by Bulat [19] as being *defined as a fraction of the intake air that is bled off and returned (or lost), and its temperature as a fraction of the compressor temperature rise. The cooling and sealing flow bled off the compressor is split in four parts (remixes) in accordance with the work done in each turbine stage. The first part (Remix 1) is assumed to enter the annulus immediately upstream of the Compressor Turbine (CT inlet), second part downstream of the Compressor Turbine (CT exit), the third part upstream of Power Turbine (PT inlet), and the last part downstream of Power Turbine (PT exit). The bleeds and remixes are defined separately*. The effect of such bleeds on overall engine performance is accounted for by reducing the amount of massflow at the exit of the compressor, and a calculation of the work requirements of the bleed air and main gas path air is done by treating both as seperate streams. The enthalpy of the bleed is used when remixing to calculate the remixed temperature [21].

MATCH offers some flexibility in design in that it can theoretically model any single spool engine, but offers no functionality to model multiple spool engines.

Academic Models

Turbomatch is a software package designed by *Cranfield University* to simulate steady state (design and off-design point) and transient performance of a gas turbine. Most applications of gas turbines (e.g. aero, industrial, simple cycle, heat recirculation) can be modelled using a highly flexibile modular approach to 'build' a engine using a number of modules (or *bricks* as they are known in Turbomatch). A detailed analysis of the operation of Turbomatch [22] is outside the scope of this report, but the primary functionality is discussed below.

Gas turbine performance is calculated by using component characteristic maps for compressors, combustion chambers, turbines (both compressor turbines and free turbines) and a map providing the velocity coefficient for exhaust nozzles. Off-design point performance is determined by using a modified Newton-Raphson method [22]. At design point mode Turbomatch provides engine performance and size data; while at off-design mode engine performance is predicted for varying throttle settings (rotational speed, combustor exist temperature, or fuel flow). Transient performance simulation is performed by controlling the fuel flow with the referred rotational speed or time. Off-design and transient calculations are based on mass and energy balance, carried out through an iterative method based on supplied component maps. A series of generic, experimentally derived maps are available within the Turbomatch scheme, or the user may elect to create a custom map. In the case of the generic maps, Turbomatch will scale them according to the design point characteristics.

To understand the modular nature of the scheme, it is first necessary to understand the modules , or 'bricks' which make up a model. Most bricks correspond to an individual gas turbine component (such as compressor, combustor or turbine), but may serve other functions (such as representing air bleeds, mixes and flow splitters). Shown in figure 2.8, each brick requires a set of input parameters. These are split between a set of mandatory thermodynamic parameters (known as Station Vectors, SV) and a set of parameters unique to that brick (known as Brick Data, BD). Outputs from the brick are passed to the next module through the mandatory station vectors. Non-mandatory outputs, such as power or thrust, are stored as *Engine Vectors* ('EV's').

Unlike MATCH, Turbomatch offers true flexibility, with nearly all gas turbine configurations ca-

pable of being modelled in the software. This does, however, increase the complexity of model design compared to other modelling tools.

Based on the criteria in table 1.1, Turbomatch is considered a *0-D* modelling tool. The ability to 'build' an engine and run it over a wide operating window without the need for detailed flow and geometrical analysis mean that it is a useful initial design phase tool. Compressor bleed is currently handled in Turbomatch in two ways; for bleed at the exit of the compressor, a 'PREMAS' brick is added post-compressor which allows for a set proportion of air to bypass the main gas path and remix at a later location using a 'MIXEES' brick. For interstage bleed, the compressor must be manually 'split' into two seperate compressors. Then, a 'PREMAS' brick is inserted in between the two pseudo-compressors and remixed back into the main gas path using a 'MIXEES' brick. This method is clearly not practical for regular use, and requires a number of assumptions to be made by the user regarding the design point parameters of both pseudo-compressors.

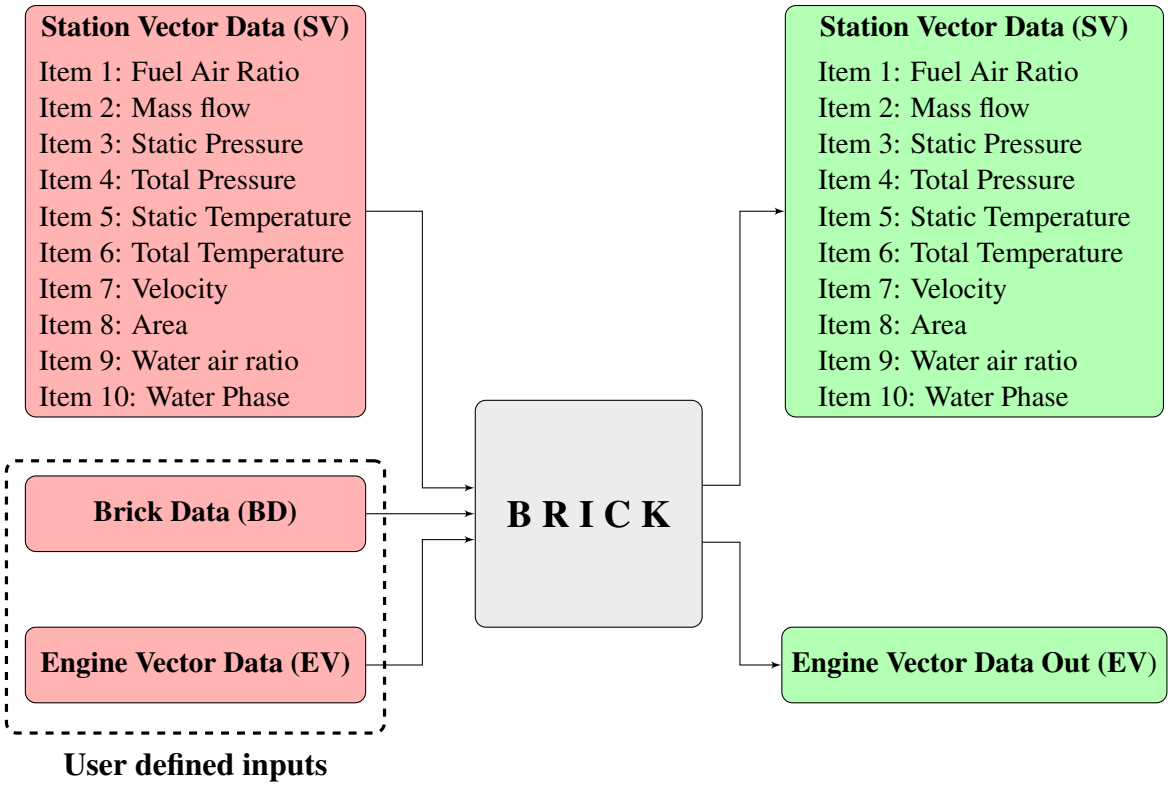

Figure 2.8: Turbomatch brick input and output

Commercial Models

There are a number of commercially available modelling tools, such as GasTurb and PROOSIS. GasTurb allows a user to select from a number of pre-determined engine configurations, and hides much of the mathematical complexity from the user. GasTurb also includes a number of useful diagnostic and analysis tools which are not strictly part of the modelling process, but are nevertheless highly useful tools. These tools and the relatively simple user inteface make it a particularly useful tool to the inexperienced user [23]. However, the lack of a full configurable engine design does restrict the flexibility somewhat. GasTurb allows bleed to be specified as both fully compressed and partially compressed flows, and these are subtracted from the net compressor flow when calculating compressor exit enthalpy [24].

GasTurb uses a term called *Relative Enthalpy Rise* [24], which is a fraction used to determine the enthalpy cost of the bleed based on the location in the compressor. This calculation is used in downstream calculations of the bleed air. It is not clear what bleed temperature and pressure assumptions are used.

Chapter 3

Validation of modelling tool

3.1 Aim

In order to demonstrate the methods shown in chapters 4 and 5, it is necessary to implement them in a modelling tool. This chapter identifies a suitable modelling tool and conducts a validation exercise using test data to investigate the suitability of the tool.

3.2 Method

There are a number of modelling tools available which are capable of modelling the gas turbine cycle (see chapter 2.5.5). However, whichever tool is selected must be able to meet the following three criteria, each of which is discussed later in more detail.

1. Have the necessary functionality to model the engine used in this study
2. Produce results which are comparable to test data
3. Are able to incorporate the alternative method, shown in figure 5.2

Based on the above criteria, the Cranfield modelling software *Turbomatch* was selected. Discussed in section 2.5.5, *Turbomatch* offers high flexibility in engine design through the construction of an engine model using 'bricks', and also offers the ability to modify the model to incorporate the alternative method proposed here through modification of the source code. Key bricks used in this modelling exercise are shown in table 3.1.

BRICK	Description
INTAKE	Specify inlet conditions such are temperature, pressure and humidity
ARITHY	Arithmetic module used to perform calculations on input and output variables. In this case, it was used to model variable inlet blade geometry
COMPRE	Gas turbine compressor. Pressure ratio, isentropic efficiency, map selection and surge margin defined here, as well as variable blade geometry position
PREMAS	Compressor bleed due to remix post-PT (i.e. exhaust duct). Primarily used for P2 bleed control
TURBIN	Module representing compressor turbine. Isentropic efficiency, enthalpy characteristics and map selection defined here
TURBIN	Module representing free power turbine. Isentropic efficiency, enthalpy characteristics and map selection defined here
MIXEES	Remix of P2 bleed air post power turbine
EXIT	Exhaust

Table 3.1: BRICKS used in SGT-400 model

3.2.1 Required functionality

Test data for this study is from the Siemens 'SGT-400' industrial gas turbine. Summarised in table 3.2, the SGT-400 is a small industrial gas turbine produced by Siemens with a single-spool, free power-turbine arrangement. First introduced in 2000, over 400 units have been sold worldwide. The product has undergone a number of design modifications over the years to improve efficiency, lifing and emissions. For each of these modifications, a *0-D* modelling tool would have been used. Such tools would also have been used for diagnostics and sales support.

Parameter	**Details**
Engine Name	SGT-400
Power	12.90MWe (power generation applications)
Power	13.40MW (mechanical applications, e.g. pumps)
Efficiency (thermal)	36.2% (mechanical applications)
Compresor stages	11
Compressor inlet air flow	38.9kg/s
Compressor stator blade modulation	Variable guide vanes for start up and speed control at full load
Compressor nominal speed	14100rpm
Compressor pressure ratio	16.8:1
Combustion	6 reverse-flow cannular combustion chambers (Dry-Low Emissions system)
Emissions control	Combustor flame management and compressor exit air bleed
Compressor Turbine	2-stage air-cooled overhung compresor turbine
Power Turbine	2-stage high efficiency turbine
Exhaust temperature	555deg. C
Year Entered service	2000

Table 3.2: SGT-400 simple-cycle performance (i.e. no waste heat recovery or combined cycle application). Details from [4].

The SGT-400 model was set up in Turbomatch as per figure 3.1, using the bricks described in table 3.1. Note that for the purposes of this example, any interstage bleed offtake is assumed to be at the compressor exit. While this undoubtedly introduces some error in the calculations, the amount of interstage bleed in the SGT-400 (at conditions other than start-up) is sufficiently small enough that the validation exercise results are not significantly affected. Once the initial validation is performed, a second validation exercise may be done using the modified bleed assumption method and the differences analysed.

In order to model the SGT-400, the user must provide a number of design point parameters, such as compressor pressure ratio, inlet and exit temperature, massflow, and isentropic efficiency. Similar parameters are required for other components in the model. The user must also select suitable compressor and turbine maps. In addition, knowledge of the specific operating characteristics is required. The SGT-400 has two characteristics which may not be immediately obvious.

Firstly, while it is not uncommon for an engine to utilise compressor stator blade modulation during start up in order to improve surge margin, the SGT-400 also utilises stator blade modulation near to full speed operating conditions. This is not for surge protection reasons, but to modulate compressor speed in order to achieve the optimum speed/massflow relationship (see figure 3.2).

Secondly, the SGT-400 utilises a method of controlling emissions by ‘bleeding’ compressor exit air to the exhaust (see section 2.3.2). Called ’turndown air’, this air effectively does no work in the engine and hence results in a higher operating temperature (hence higher flame temperature), for a given load. This enables CO emissions to be minimised for off-design running. This is controlled by adjusting the turndown air outlet valve to maintain a constant operating temperature until a maximum valve angle is achieved (see figure 3.2). Note this is a seperate air-offtake to typical bleed air used for blade cooling and secondary systems.

While not necessary for design point simulation, knowledge of both these control methods is essential in order to properly model the engine in Turbomatch at off-design conditions. Fortunately, Turbomatch provides the necessary functionality to account for these control schemes. As turndown air is a post-compressor offtake, it can simply be controlled by the use of an ‘PREMAS’ brick after the compressor, but pre-combustor. It is then remixed back into the gas path in the exhaust using a ‘MIXEES’ brick. The variable geometry is accounted for by implementing a non-

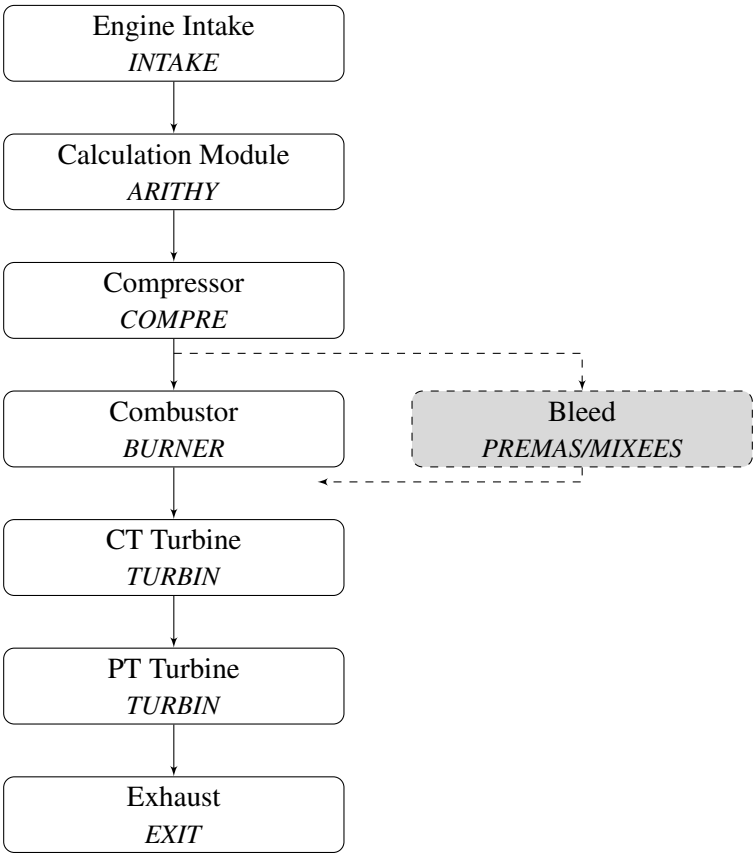

Figure 3.1: SGT-400 arrangement using Turbomatch. Text in *italics* represent Turbomatch module names.

dimensional VGV schedule into Turbomatch using the ARITHY module, based on a range of 1 (fully open position) to 10 (fully closed position). As modulation of the VGVs on a free power turbine engine will cause a change in speed (and hence massflow) at the same operating condition, investigating the change in massflow will give a good indication of the accuracy of VGV map.

3.3 Other cycle considerations

As all SGT-400's are tested at the Siemens Lincoln in-house test facility, detailed performance data is available for comparison with Turbomatch. For the purposes of this investigation, the results taken from an engine factory test in May 2017 are compared to the two methods above. Design point performance has been defined as running at full power at ISO conditions (table 2.2). Ducting losses are calculated based on the measured pressure differential in the inlet and exhaust, and gearbox losses are based on manufacturers data sheets. Also note that windage and bearing power

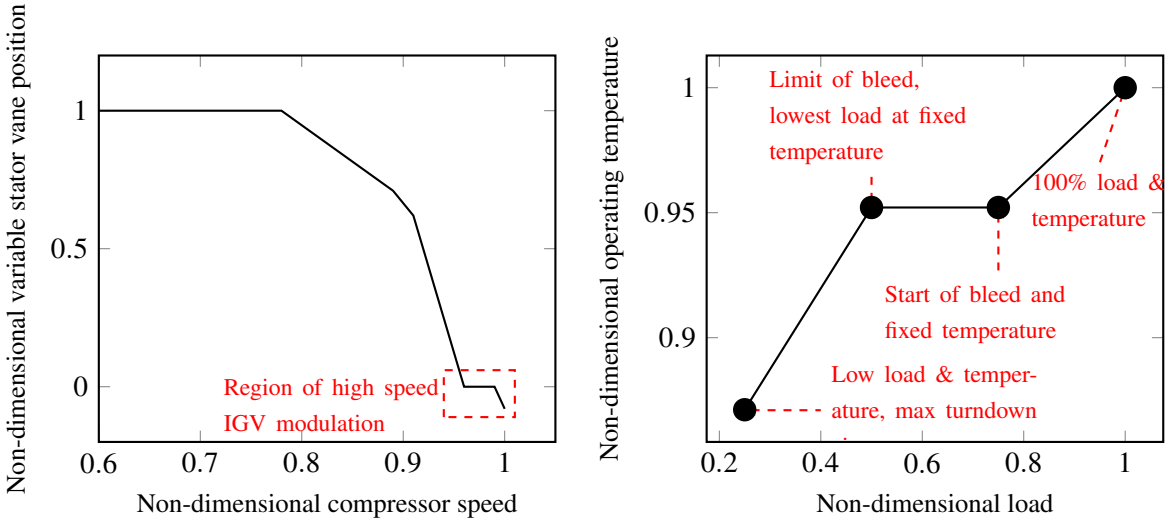

Figure 3.2: Speed / variable stator blade relationship, and turndown air - SGT-400

loss are based on Siemens design assumptions. Similarly, secondary air system flows are based on engine flow models. Fuel composition falls within typical definition of natural gas (*naturally occurring methane with no more than 20% (by volume) of inerts and other constituents* [25]). These main parameters are shown in table 3.3.

3.4 Measurement Uncertainties

It is beyond the scope of this report to conduct a full error analysis of the test results. However, previous investigations by Siemens, recorded in internal test reports [26], suggest that typical uncertainties in power, temperature, air mass flow, fuel mass flow and thermal efficiency are around 0.5% to 0.8%. Pressure measurements tend to be more accurate, with a typical uncertainty of 0.1%. While these values can't be used to directly assess the difference between model and test results, they do offer a useful baseline comparison.

3.5 Design Point Analysis

Table 3.4 shows a comparison of real test data and TurboMatch at design point (defined as the same Turbine Entry Temperature as full power conditions of the test engine). Power, mass flow, compressor exit pressure, compressor speed, and interduct temperature show agreement within ±

Parameters	**D.P. Value**
'Design point'	
Ambient conditions	ISO
(Normalised) Turbine Entry Temperature	1.0
Mass flow	39.56kg^s
Pressure ratio	17.34
Assumed combustor pressure loss	4%
Combustor efficiency	100%
Free power turbine speed	100%
Mechanical losses	
Gas generator bearing losses	assume 4%
Gas generator windage losses	
Power turbine bearing losses	
Power turbine windage losses	
Casing heat losses	
Inlet duct losses	none
Exhaust duct losses	none
Gearbox efficiency	100%

Table 3.3: Test engine design point parameters

0.5%. Thermal efficiency, heat input and exhaust temperature are within approximately $\pm$ 1.5%. If the typical measurement error on these parameters is around $\pm$ 0.8%, then these results show Turbomatch compares well with test data. The reasons for these deviations are discussed in more detail the next section.

However, design point conditions are relatively simple to model (certainly compared to off-design), and do not require map scaling or interpolation. Similarly, the control methods from figure 3.2 are not in operation at the design point. For off-design performance calculations, certain quantities have to be varied to match mass continuity, shaft speed and power balance. These are known as *variables*. The number of variables and errors is fixed by the nature of the engine cycle (i.e. engine configuration, or the bricks used in the model). One or more of these variables are defined during off-design analysis as a 'target', or engine 'handle' - in other words, the user specifies a fixed value of the variable defined as the handle, and the software runs through an iteration loop until the value of the variable is satisfied.

Parameter	Difference
Output power	0.5%
Thermal efficiency	-1.4%
Turbine Entry Temp.	0.0%
Mass flow	0.0%
Compressor exit pres.	-0.5%
Compressor exit temp.	1.3%
Compressor speed	0.0%
Fuel flow	-3.2%
Heat input (MW)	1.9%
CT/PT interduct temp.	-0.5%
Exhaust temp.	-1.7%

Table 3.4: Test engine. Real data vs. Turbomatch at design point, DP

3.6 Results

Using Turbine Entry Temperature (equivalent to $T4$ in ARP nomenclature) as a handle, off-design performance for the test engine was run at the following conditions:

1. TET= $(designpoint - 24K)$, No turndown air (97% load)
2. TET= $(designpoint - 30K)$, No turndown air (93% load)
3. TET= $(designpoint - 56K)$, 3.1% turndown air (75% load)
4. TET= $(designpoint - 48K)$, 11.5% turndown air (48% load)

Note that for 75% and 48% load points, turndown air was in operation, thus maintaining TET in a $20K$ range for emissions control. Stator blade modulation was in operation for all points.

Results are shown in figure 3.3 and are compared to test data. Power (a), thermal efficiency (c), air mass flow (d), compressor pressure ratio (e) and CT/PT interduct temperature (f) show excellent agreement - less than 0.5%, which is well within any measurement uncertainties from the test instrumentation, rising to around 1-2% for the final (low load) test point. It is interesting to note that the comparison for thermal efficiency (c) actually *improves* after the initial design point (from around 1.5% to 0.5%). Fuel flow (b) is a little less accurate (around 3%), which is likely due to the different calculation methods between the test data and Turbomatch calculations. Fuel flow from the test data has been measured using a coriolis massflow meter, which will have an

associated uncertainty of up to 1%. The Turbomatch data, however, calculates fuel flow based on the thermodynamic (calculated) heat input into the engine and a generic fuel calorific value. This calorific value is likely to be different to the actual value on test, and hence will contribute to some of the uncertainty. As discussed in chapter 5, locating all bleed at the exit of the compresor may also have introduced some error.

Exhaust temperature, however, shows a consistent difference of around 10 degrees across the load range, which is likely to be due to the mixing of some of the secondary air flows into the exhaust, which may be modelled differently in Turbomatch compared to the actual engine. However, the relatively consistent delta between Turbomatch and Test data (of around 10 degrees), as well as the more accurate agreement in interduct temperature suggest that this is a minor issue.

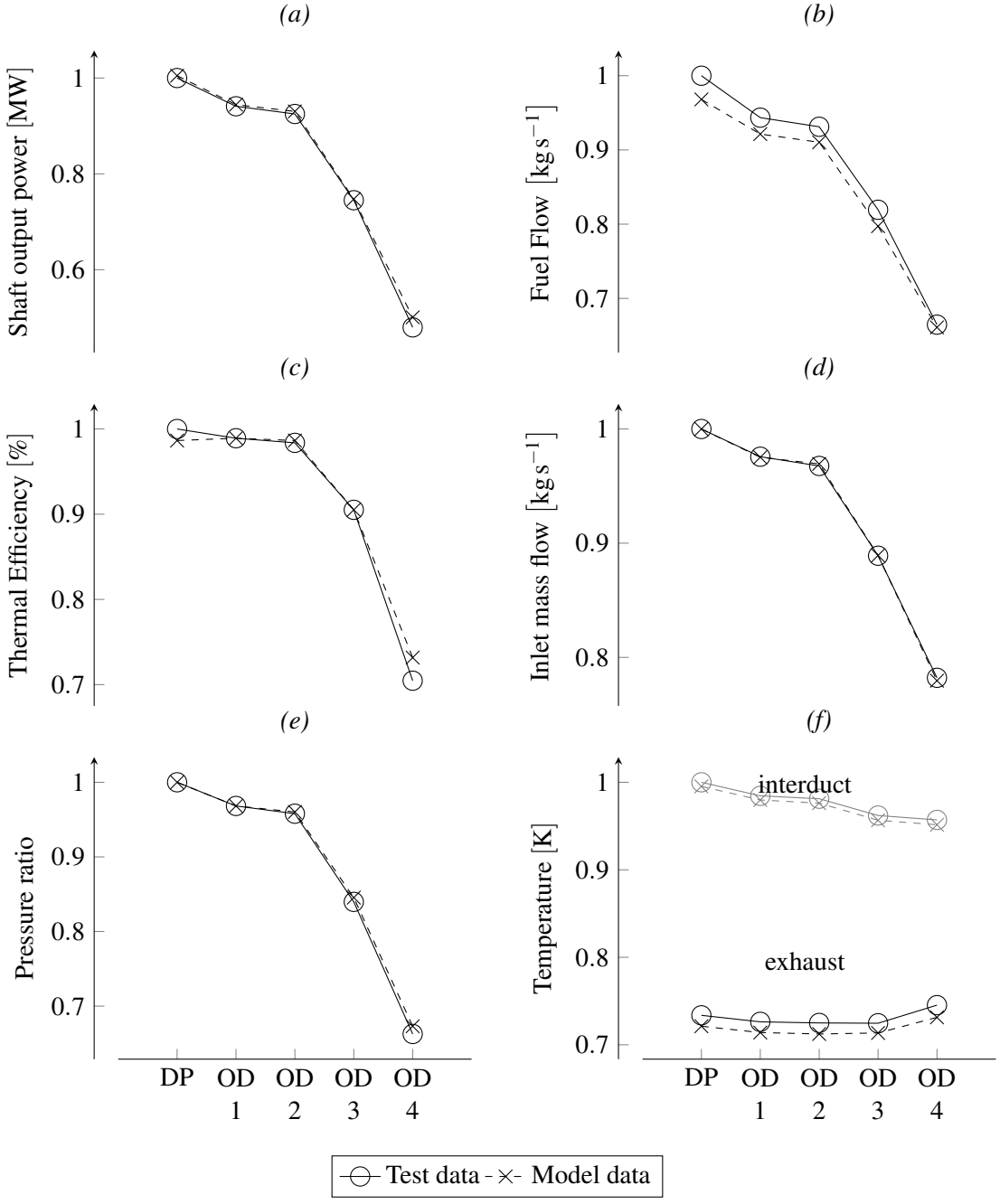

DP= Design Point
OD1 = TET= $(designpoint - 24K)$, No turndown air (97% load)
OD2 = TET= $(designpoint - 30K)$, No turndown air (93% load)
OD3 = TET = $(designpoint - 56K)$, 3.1% turndown air (75% load)
OD4 = TET= $(designpoint - 48K)$, 11.5% turndown air (48% load)

Figure 3.3: TurboMatch vs. Test data for selected output parameters

3.7 Analysis

The results in figure 3.3 show a difference between test and model data of around 0.5%-1% for the main performance parameters of power, fuel flow and thermal efficiency. Furthermore, compressor inlet mass flow and pressure ratio show good agreement. The differences between test and model data can easily be accounted for by consideration of test measurement uncertainties, the difference in fuel composition, and exhaust remixing. The results show that Turbomatch performs well in predicting gas turbine steady state performance at both design and off-design conditions, even when using one (of five) generic compressor and turbine maps, rather than a product specific map. Furthermore, the design of Turbomatch makes it well suited for future modifications through the addition of new modules.

Chapter 4

Derivation of bleed flow, pressure and temperature

4.1 Aim

Compressor bleed air is used for a wide range of functions (see table 2.4). It is therefore important that the properties of the bleed air – specifically mass flow, pressure and temperaure, are known. Asuuming that the amount of masflow at the bleed is known, a method is shown in this chapter that demonstrates how temperature and pressure may be calculated using design assumptions and design-point data.

Note that in the following chapters, engine station numbers are based on the ARP standard [5], as shown in figure 1.2.

4.2 Working fluid assumptions

Any investigation into the effect of bleed on compressor and engine performance must require knowledge of the properties of the working fluid (usually air, or air and fuel). Of particular use are the specific heat capacities, C_v and C_p, as these are used directly in some calculations or as part of the gamma (γ) calculation. For demonstrative purposes within this report, a simple polynomial equation (from Walsh and Fletcher [10]) for C_p combined with a crude estimation of the gas constant R is used. However, any model results presented within the report use a much more rigorous method detailed by Bucker [27], which enables C_p, enthalpy (H) and gamma (γ) to be calculated for a range of working fluids and water contents. This method is too complex to describe within this report and for practical uses requires programmatically solving.

4.3 Derivation of stage temperature rise

4.3.1 Method

It may be assumed that the following design-point characteristics are known to the user, or in the case of off-design analysis, have been calculated by the modelling software:

- Compressor inlet temperature
- Compressor inlet pressure
- Compressor exit temperature
- Compressor exit pressure
- Bleed massflow (usually as a fraction on inlet flow)
- Overall compressor isentropic efficiency

This is not an unreasonable assumption to make. If analysing at design point, all the above factors will be pre-defined. If not at design point, then the compressor map may be used to derive off-design conditions (in reality this is done programmatically using an iterative process).

As bleed air is often used for downstream secondary systems, such as bearing sealing, turbine blade cooling, bearing thrust modification or cabin pressure air [12], knowledge of the temperature and pressure of the bleed air is required. It is also required in order to calculate bleed work and enthalpy. Pressure and temperature at the bleed point may be calculated using a simple assumption that it is equal to the compressor exit temperature and pressure. Such an assumption, however, would introduce unacceptable errors in the cycle calculation, as any remixed air would have an artificially high enthalpy and would overestimate the contribution of the bleed air to useful work. A more practical solution is to assume that the compressor stage pressure rise (δ) and temperature rise (ζ) is linear and uniform through the compressor. In other words, temperature rise may be expressed as:

$$\zeta = (T_3 - T_2)/n_{last} \tag{4.1}$$

and pressure rise per stage may be expressed as a function of inlet pressure and overall compressor

pressure ratio (Π_{comp}):

$$\delta = (P_2 \times (\Pi - 1))/n_{last} \tag{4.2}$$

4.3.2 Results

In order to establish whether linear temperature and pressure rise is a reasonable assumption, an investigation of six Siemens industrial gas turbines of varying technology levels designed over over a 30 year period was undertaken. Shown in table 4.1 it can be seen that older engines typically had lower pressure ratio, lower polytropic efficiency and subsonic blade axial velocities. These engines typically had the 'C4' style compressor rotor blades while the more modern engines use DCA or MCA style compressor blades (see section 2.3.3).

Note that table 4.1 defines component efficiency in terms of polytopic rather than isentropic efficiency. In terms of overall component efficiency, the overall compressor *isentropic* efficiency cannot be assumed to represent the stage efficiency (see section 2.4.1).

Figure 4.1 shows normalised temperature and pressure rise for these engines for each stage of the compressor (normalised so that the different pressures and temperatures can be compared).

Engine Ref	**SGT100E**	**SGT-300**	**SGT-400**	**SGT100**	**SGT200**	**TB5000W**
Modelling tool	CFXv14.5	TFLOW	CFD	CFXv14.5	MEPALP	TFLOW
Approx. Introduction	2012	2007	2000	1998	1982	1983
Blade technology level assumed	3D MCA	DCA/C4	DCA	DCA	C4	C4
Actual blade technology level	3D MCA	3D MCA	DCA	DCA	C4	C4
Relative Velocity	Transonic	Transonic	Transonic	Transonic	Subsonic	Subsonic
Blade stages	10	10	11	10	15	13
Speed (100%) [rpm]	17384	14010	14300	17384	11085	10750
Pressure ratio	0.919	0.819	1.000	0.836	0.702	0.556
Overall polytropic efficiency	1.000	0.997	1.003	0.997	0.968	0.959

Table 4.1: Engine details. Note that pressure ratio and overall polytropic efficiency are expressed non-dimensionally as a function of the highest respective value of the engines compared

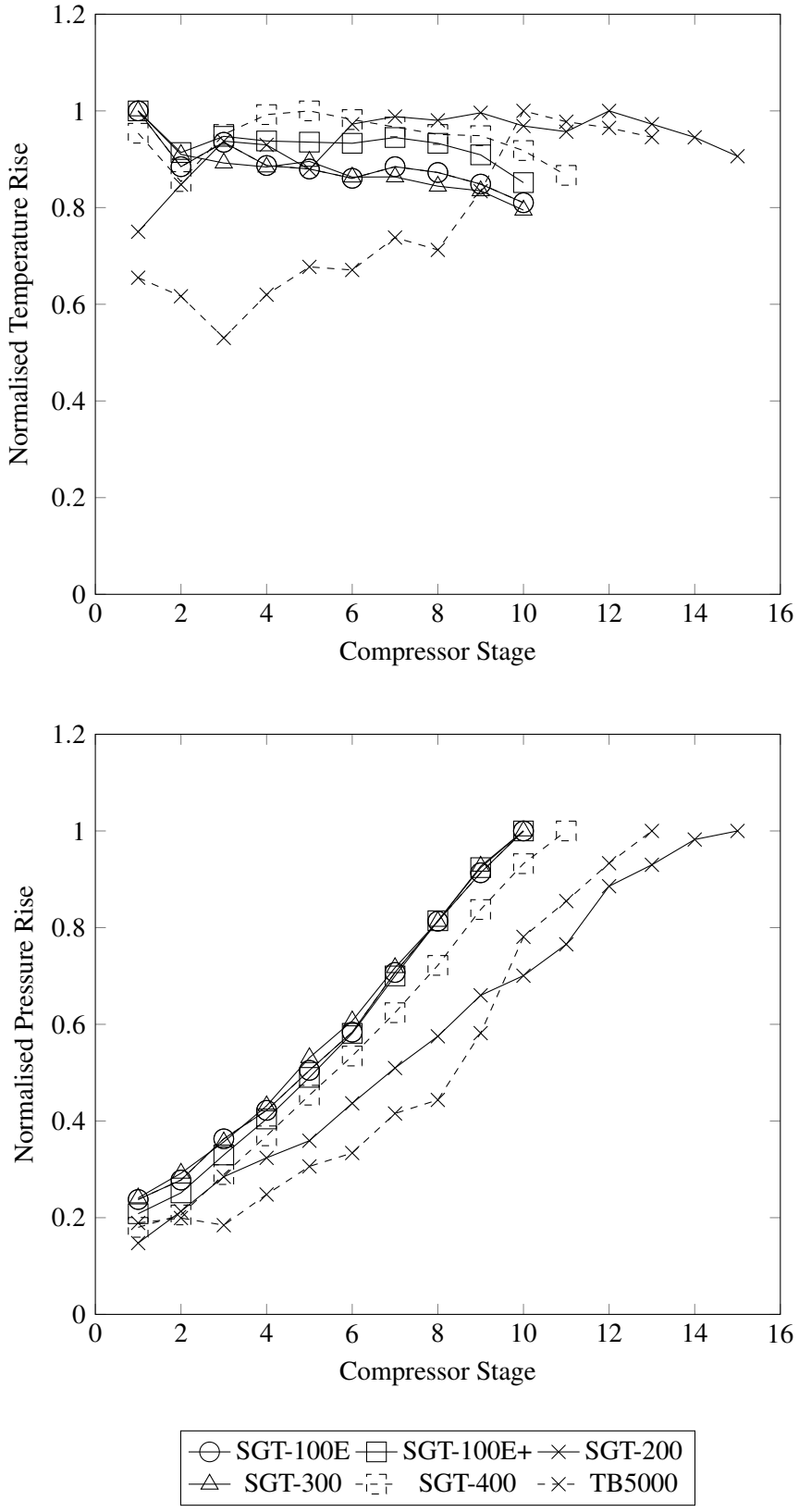

Figure 4.1: Pressure and Temperature rise per stage. Values are shown relative to the maximum for each engine (i.e. current value / maximum value)

4.3.3 Analysis

It can be observed that temperature rise is broadly constant from stage to stage for all engines (stage temperature rise is within 0.9 ± 0.1 for all stages), and hence it is not unreasonable to assume a linear temperature rise per compressor stage. The only exception to this is the 'TB5000', which shows much more variation in stage temperature rise (0.8 ± 0.2), although it should be noted that the TB500 represents the oldest technology level in the study (original variants were built in the 1970's). The other engine types in this study share a more common (modern) technology level.

However, normalised *pressure* rise is not constant nor linear for any of the engines in the study. Another method to obtain stage pressure rise must be used.

4.4 Derivation of stage pressure rise

4.4.1 Method

Normalised polytropic efficiency (figure 4.2), is observed to be broadly constant across compressor stages, and is within 0.99 ± 0.05 normalized efficiency for all engines aside from the TB5000E, which has a normalised efficiency range of 0.95 ± 0.05. Interestingly, both the TB5000E and the SGT-200 (the oldest technology engines in the study). appear to have a decline in polytropic efficiency at the front stage and towards the later stages, but are relatively consistent with the other engines for all other stages. This may be due to different loading on the front and rear stages associated with the older blade technology levels.

The assumption is made that the overall compressor polytropic efficiency can be used to represent stage polytropic efficiency (which is not unreasonable as the very definition of polytropic efficiency is the 'small-stage' efficiency), and combined with the assumption of linear temperature rise per blade stage, can be used to calculate stage pressure rise. Design point compressor exit temperature, pressure ratio and efficiency are likely known for nearly all modelling methods. It is a relatively simple task to establish stage temperature assuming constant temperature rise.

Pressure rise using polytropic relationship

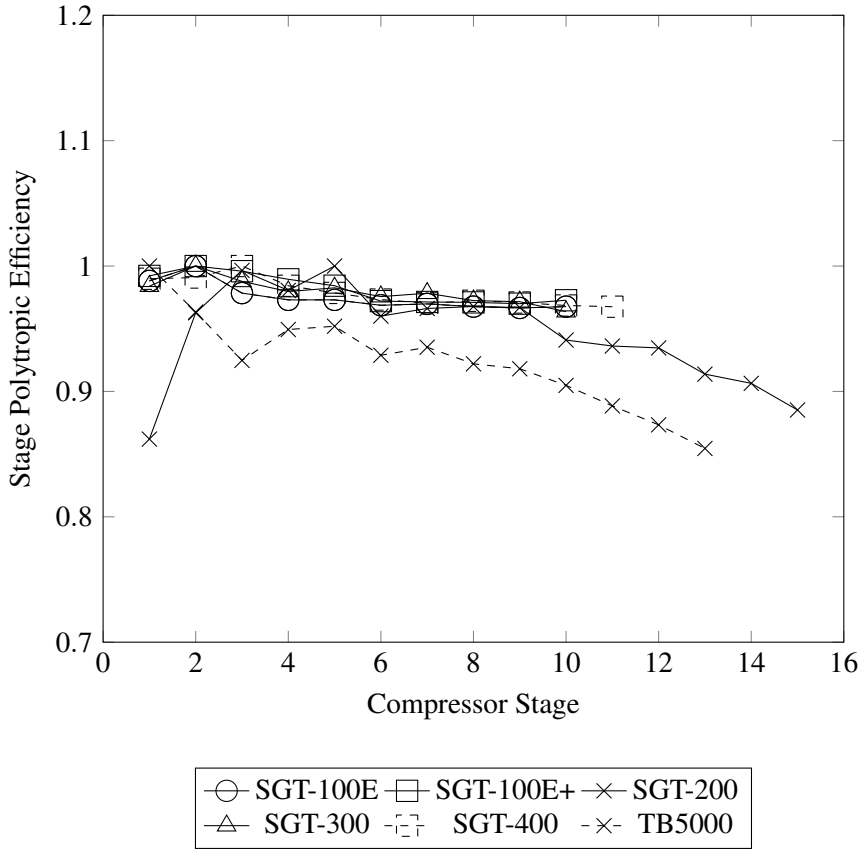

Figure 4.2: Polytropic efficiency per stage. Values normalised to peak value for each engine

Using the expression for polytropic efficiency [1]:

$$\eta_{poly} = \frac{\ln\left(\Pi_{comp}\right)^{\left(\frac{\gamma-1}{\gamma}\right)}}{\ln\left(\frac{T_3}{T_2}\right)} \tag{4.3}$$

where Π_{comp} is overall pressure ratio, T_3 is compressor exit temperature and T_2 is compressor inlet temperature. Re-arranging in terms of stage pressure ratio (π_n) gives the following:

$$\pi_n = \left[1 + \left(\frac{\zeta}{T_{in}}\right)\right]^{\eta_{poly}\left(\frac{\gamma}{\gamma-1}\right)} \tag{4.4}$$

where ζ = stage temperature rise:

$$\zeta = (T_3 - T_2)/n_{last} \tag{4.5}$$

This in turn may be used to estimate stage pressure rise assuming constant temperature rise.

4.4.2 Results

A step-by step example of this method on an SGT-400 is shown in appendix A, and figure 4.3 shows the application of this method to all the engine examples in table 4.1. Also plotted on each graph is the assumed pressure per stage using the very simple assumption that pressure rise is linear and equal across all stages.

4.4.3 Analysis

The results suggest that using the proposed method of deriving stage characteristics, stage pressure is within 3% of the baseline results for all engines aside from the TB5000E, which shows a slightly larger difference. As the TB5000E represents the lowest technology level, improvements to the stage characteristic assumptions could be made to accommodate these lower technology engine designs, although the accuracy is still greater than a linear pressure rise assumption. Based on these results, it has been decided that the polytropic efficiency-derived pressure is sufficiently accurate (and certainly more accurate than linear pressure rise assumptions) such that it can be used in bleed calculations.

Note that an alternative way of calculating stage pressure rise is by making the assumption that the overall stage *polytropic* efficiency is roughly equal to the individual stage *isentropic* efficiency. While it has been established that the difference between isentropic and polytropic efficiency increases with pressure ratio, for small pressure ratios the polytropic and isentropic efficiency are similar. For example, the 11 stage compressor in the GE9X aero engine has one of the highest pressure ratios in the world (27:1, which is approximately a pressure rise of 2.5:1 per stage) [28], and by analysing figure 2.7, it is seen that a modern compressor with a stage pressure rise of 2.5:1 would have a difference of 1% between polytropic and isentropic efficiency. While this would be an unacceptable error to use in analysis of the overall compressor performance, it may be small enough to provide an accurate enough approximation of stage pressure rise.

By applying a similar method to that used in equations 4.3 and 4.4, but using the isentropic efficiency expression (equation 2.9) rather than polytropic efficiency, an estimation of the stage pressure rise has been made using the SGT-400. Results are shown in appendix B and show that

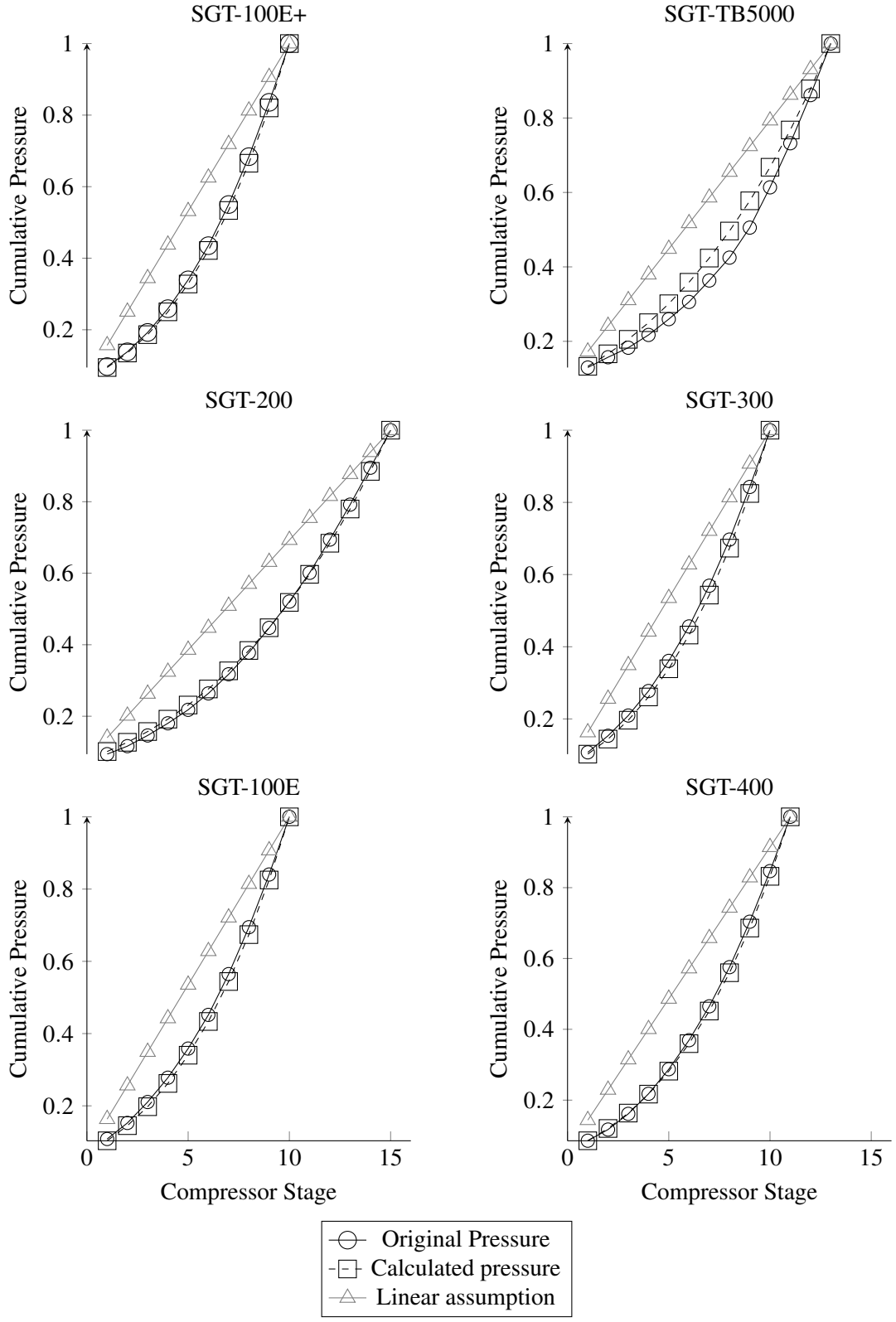

Figure 4.3: Pressure rise per stage comparison. Values are normalised to maximum pressure

the difference between the two methods is very small (around the same order as the polytropic results). However, the polytropic method has been selected as the method to be implemented as there is evidence within this report showing that a constant stage polytropic efficiency is a reasonable assumption (see figure 4.2). This is not to say there is no merit in the isentropic method, but more research should be done before adopting it.

Chapter 5

Derivation of compressor work and overall cycle change

5.1 Aims

Chapter 4 describes a method for calculating bleed temperature and pressure. However, it is equally important to be able to model the effect of bleed on both compressor work requirements and the overall gas turbine cycle. This chapter derives a method for doing this, and uses the modelling software identified in chapter 3 to validate this method.

Station numbering is as per figure 1.2

5.2 Theory

Considering a case where there is no compressor bleed, the work required to drive the compressor, or the *power absorbed* by the compressor can be defined as the change in enthalpy between compressor inlet and exit. Change in enthalpy (Δh) is expressed as:

$$\Delta h = (C_p T)_3 - (C_p T)_2 \tag{5.1}$$

Assuming constant specific heat capacity C_p:

$$\Delta h = C_p(T_3 - T_2) \tag{5.2}$$

The power absorbed ($\dot{W}$) is therefore the change in enthalpy times unit mass flow

$$\dot{W}_{3-2} = \dot{m}_2 C_p(T_3 - T_2) \tag{5.3}$$

The work for the compressor is provided by the compressor turbine. Turbine power is calculated in the same way as compressor work, although in the case of a single spool turbine (i.e. power generation unit) the work produced by the turbine is equal to compressor work plus useful output work. In the case of a free power turbine engine, compressor turbine work must equal compressor work. In reality, there are a number of losses to consider within the compressor (e.g. bearing losses or windage losses), but for simplicity these are ignored in the equation below (but are included in the modelling exercises conducted within this report).

$$\dot{W}_{4-3} = \dot{W}_{3-2} + losses \tag{5.4}$$

For the first approximation, the introduction of bleed at stage n, where $n = blade\ stage\ in\ compressor$, is ignored. However, the reduction in air mass flow will in reality result in a change to the power absorbed by the compressor. As bleed represents a reduction of flow from the compressor, and hence a reduction in the amount of mass flow which has work done on it (from the bleed stage onwards), the change in compressor work can be calculated by firstly calculating the work which *would have been done* on the bleed air had it remained part of the main gas path. In summary:

For bleed quantity $\dot{m}_{21}$ at stage n:

1. Work is still done on $\dot{m}_{21}$ from compressor stages 1 to n
2. Work is no longer done on $\dot{m}_{21}$ from compressor stage $n+1$ to the exit of the compressor
3. Thus the change in compressor work can be defined as *the original no bleed work minus the work which is no longer done on the bleed air*

$$\Delta\dot{W}_{3-21} = \dot{m}_{21} C_p (T_3 - T_{21}) \tag{5.5}$$

Hence new compressor work is essentially the original work calculation minus the work which is no longer done on the bleed air (equation 5.3 minus equation 5.5). This revised value of work and massflow is then passed to the modelling software and the next iteration can occur. This will then result in a change to the matching conditions of the engine and hence different compressor exit

temperature and pressure, and overall cycle performance.

$$\dot{W}_{3-21} = [\dot{m}_2 C_p(p(T_3 - T_2] - [\dot{m}_{21} C_p(T_3 - T_{21})] \tag{5.6}$$

Equation 5.6 shows that bleed air actually *reduces* the power absorbed by the compressor. It therefore stands to reason that the lower the value of n, the greater the benefit from not doing work on the bleed air. Note that in terms of *overall performance* of the gas turbine, the reduction in compressor work is clearly offset by the reduction in useful mass flow through the combustor. This leads to the theory that the further along the compressor the bleed is, the less 'benefit" from not having to do work on it, and conversely the more bleed at bleed stage n, the greater the reduction in compressor work required. This can be expressed as

$$for \quad \dot{m}_{bleed} = C, \quad \dot{W}_{comp} \propto n_{bleed} \tag{5.7}$$

and

$$for \quad n_{bleed} = C, \quad \dot{W}_{comp} - \propto \dot{m}_{bleed} \tag{5.8}$$

Equations 5.7 and 5.8 show the reduction of compressor work as a result of bleed. Taking the compressor as an isolated system, this means that less work must be provided to the compressor and hence more useful work is available for thrust or power. However, the compressor cannot be considered an isolated system, and ultimately the effect of bleed is that less air is provided to the combustion system and hence less energy produced, even when considering bleed remixing in later stages of the turbine. This must result in a net loss of performance, as shown in the magnification of the compression stage of the Brayton Cycle (figure 5.1). The main gas path air follows the typical real process *1-2-3-4* (*1-2'-3-4'* representing the ideal cycle). The bleed air will follow the same real compression process as the main gas path from *1-2* until it reaches the stage where the bleed air is offtaken (represented by *1B'* in figure 5.1). There is no combustion of this bleed air (so no equivalent of stages *2-3*), but there will be expansion upon remixing into the turbine (represented by *1B"*). It can be seen that $\Delta(1 - 1B') > \Delta(1B' - 1B'')$, thus showing that bleed offtake will always result in a net loss of overall efficiency compared to a no-bleed case, and hence a net loss of shaft output power.

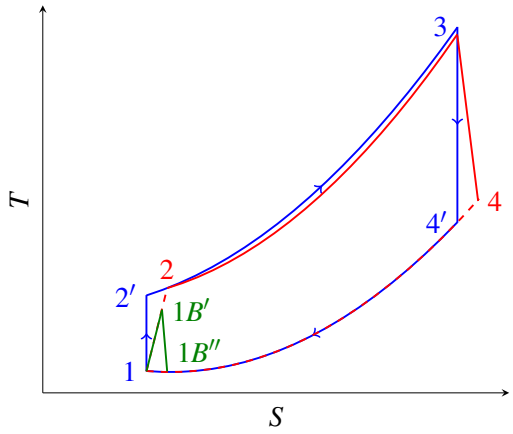

Figure 5.1: The Brayton cycle, including bleed

In addition, a case study for illustrative purposes only is shown below. This case study does not account for cycle matching changes, so its relevance to the gas turbine cycle is limited. The 'best case' scenario (in terms of extracting the maximum energy out of the bleed air) is used in this example where bleed is remixed into the gas path immediately prior to the first stage turbine.

Energy into the turbine is a result of energy from combustion plus the remix of bleed air (note simplified assumptions of fuel heat input are made in this example):

$$\dot{Q}_4 = \dot{Q}_{fuel} + \dot{Q}_{21} \tag{5.9}$$

Where

$$\dot{Q}_{fuel} = \dot{m}_{fuel} C_p (T_4 - T_3) \tag{5.10}$$

$$\dot{Q}_{21} = \dot{m}_{21} C_p (T_{21} - T_2) \tag{5.11}$$

Thus for the example parameters in table 5.1, which represents a small industrial gas turbine with 2% bleed at compressor stage 6 (of 11), net surplus power available has been calculated where $bleed = 0$ and $bleed = \dot{m}_{bleed}$ and presented in table 5.2. This shows an approximate net 'cost' of 400kW using bleed.

Parameter	**Unit**	**Value**
T_2	K	288.0
T_3	K	700.0
$T_{21'}$	K	500.0
T_4	K	1600.0
$C_{p_{2-3}}$	J/Kg.k	1.075
$C_{p_{4-41}}$	J/Kg.K	1.220
$\dot{m}_{fuel}$	kg/s	0.8
$\dot{m}_2$	kg/s	32.0
$\dot{m}_{21'_n}$	kg/s	0.8

Table 5.1: Example of energy into turbine change

Parameter	$bleed = 0$ ($\dot{m}_{exit} = 32.0$)	$bleed = \dot{m}_{bleed}$ ($\dot{m}_{exit} = 31.2$)
$\dot{W}_{compressor}$	14173kW	13818kW
$\dot{Q}_{bleed}$	0kW	182kW
$\dot{Q}_{combustor}$	36014kW	35136kW
Net turbine in	36014kW	35318kW
Net useful work	21842kW	21500kW

Table 5.2: Difference in net surplus work

This leads to the theory that bleed will always result in net loss of shaft output power, and increasing the amount of bleed will have greater negative effect than increasing the bleed stage. In order to validate these methods, it is necessary to incorporate them into a modelling tool.

5.3 Method

Known as COMPRE within the TurboMatch programming environment, the compressor subroutine is designed to calculate the outlet conditions and work from a compressor given the inlet conditions, design-point pressure ratio and isentropic efficiency, and off-design values of the relative non-dimensional speed and distance from the surge line.

The method proposed in this chapter and chapter 4 may be applied to a compressor model through the following process:

1. Establish the no bleed case for pressure, temperature, massflow and work. Identify isentropic (or polytropic) efficiency. Convert overall isentropic efficiency to overall polytropic efficiency if required. This will be performed for each iterative cycle of the modelling software
2. Identify the current bleed location, bleed massflow, and number of stages in the compressor (set by the user in the input file).
3. Calculate overall compressor polytropic efficiency based on temperatrure and pressure ratio from the no-bleed case. Gamma is obtained from software working fluid subroutines.
4. Artificially (and within the bleed routine only) split compressor into number of stages specified. Assume equal temperature distribution.
5. For each stage, calculate pressure ratio using polytropic efficiency expression and equal temperature distribution.
6. Establish pressure, temperature and massflow for the bleed stage.
7. Calculate enthalpy at compressor inlet, compressor exit, and at bleed.
8. Calculate new compressor work based on the work done in no-bleed case minus the works which *would have been done* by the massflow exiting at the bleed offtake.
9. Feed back new thermodynamic parameters into compressor subroutine
10. Repeat for each bleed specified.

11. Proceed to next main subroutine iteration.

By using the theory presented in chapter 4 to obtain compressor bleed pressure and temperature, and the methods in chapter 5 to calculate the change in compressor work, the effect of bleed on the overall gas turbine cycle may be investigated. The combination of these two methods can be implemented using the process described in figure 5.2.

Basic on this logic, the Turbomatch code has been altered such that interstage bleeds may now be modelled, and correspondingly a revised compressor work and massflow are calculated. In addition, massflow and temperature of the bleed(s) are output and (if required) remixed using a modified MIXEES brick. Up to three interstage bleeds may be modelled.

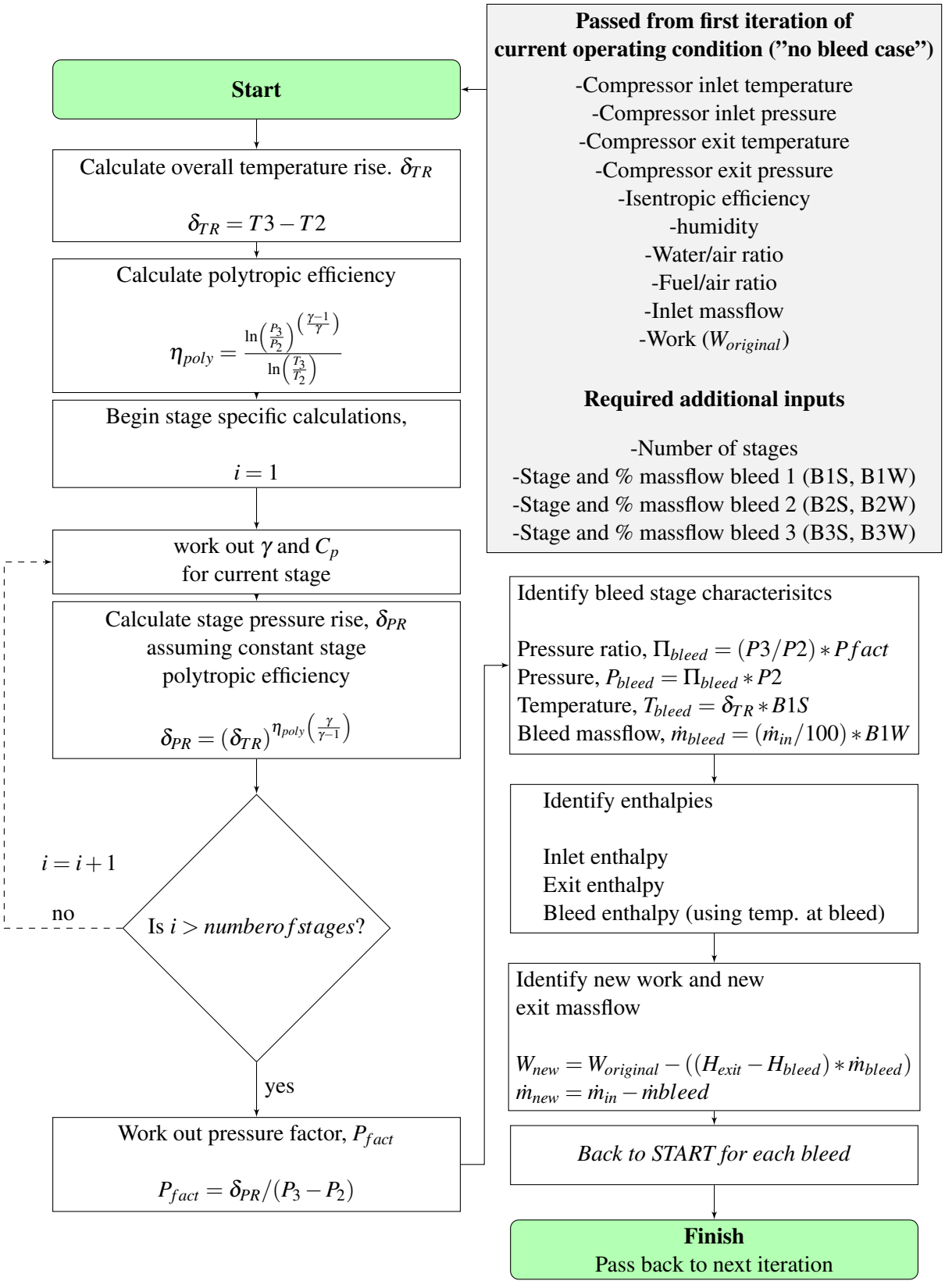

Figure 5.2: Flowchart showing new bleed methodology

5.3.1 Validation of new code

As code changes have been made to the modelling software, it is important to check that any change in the calculations are those intended by the introduction of the new method only (i.e. to check the code has not been inadvertently changed in another way). Therefore the new Turbomatch code has been validated by modelling the same engine used in the initial validation case with the same input parameters and bleed assumptions (i.e. **not** utilising the new bleed options).

Results (see figure 5.3) show that the largest difference between the 'old' and 'new' code is 0.014%, which was seen on relative stator angle stator. All other differences were below 0.005%. Such differences are minor, and show that the 'old' and 'new' code are functionally the same when the new interstage bleed functionality is not used in the new version.

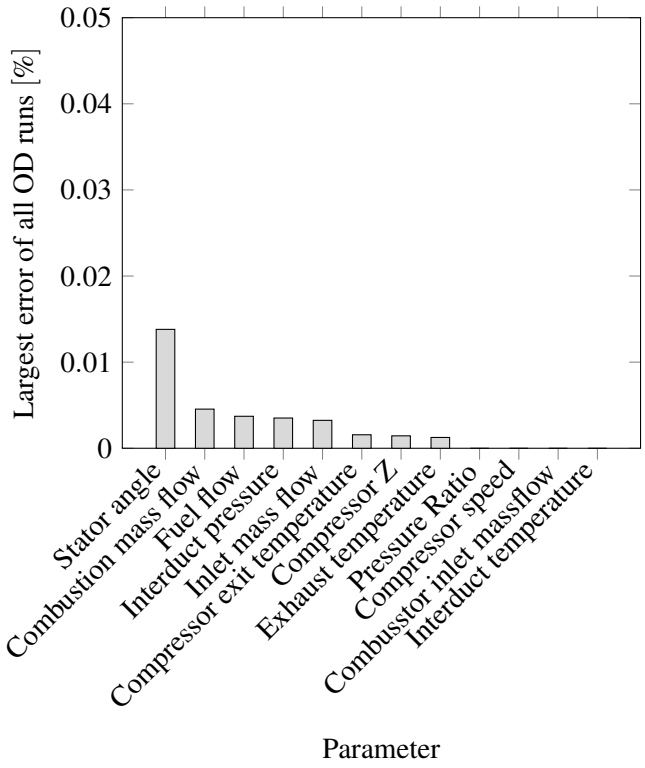

Figure 5.3: Worst case errors (%) between 'new' and 'old Turbomatch

5.4 Results

5.4.1 Theoretical comparisons

In order to investigate the theory presented in equation 5.7:

(a) *The further along the compressor the bleed is, the less 'benefit" there is from not having to do work on it*

and:

(b) *The more bleed at bleed stage n, the greater the reduction in compressor work required*

and the theory presented in equation 5.8:

(c) *Bleed will always result in net loss of shaft output power, and increasing the amount of bleed will have greater negative effect than increasing the bleed stage.*

some initial trial runs were done using the alternate method. Following validation of the new code, two test cases were run:

1. **"Varying Stage Case"**. Varying bleed stage between 1 and 11, using the same amount of bleed each time. In this case, compressor exit mass flow and bleed mass flow are constant.
2. **"Varying Bleed Case"**. Varying bleed amount between 0 and 10% at a fixed stage. In this case, the temperature and pressure at the fixed bleed stage are constant..

For the *varying stage* case (figure 5.4), bleed temperature *(c)* follows a linear trend, and pressure *(d)* follows the trend defined by use of the polytropic efficiency, showing that the implementation of the methods discussed in chapter 4 is working as intended. Of more interest are the plots of shaft output power *(a)* and compressor work *(b)*. It can be seen that by varing bleed stage from 1 to 11 (exit), shaft output power is reduced by 1%. Compressor work increases by approximately

2% from first to last stage. This is unsurprising as with increasing bleed extraction stage, more and more work is done on that bleed air that is ultimately not used in the main gas path. So, while there is no change to the bleed massflow. the results show that by increasing the stage the engine efficiency is reduced.

For the *varying bleed* case (figure 5.5), bleed pressure and temperature remain constant, as the bleed stage is not changing. Obviously, as bleed air mass flow increases *(d)*, compressor exit massflow *(c)* reduces. Interestingly, while the reduction in massflow reduces compressor work requirements by up to 4% (meaning less work is required to drive the compressor), the net output power *(a)* is also reduced. In fact, the reduction in output power is around 8% - significantly more than the reduction seen in the the varying stage case.

Both cases show that shaft output power is reduced compared to the no-bleed case. The results also show that the power loss is clearly greater in the varying bleed case. These observations are in line with the theories presented above.

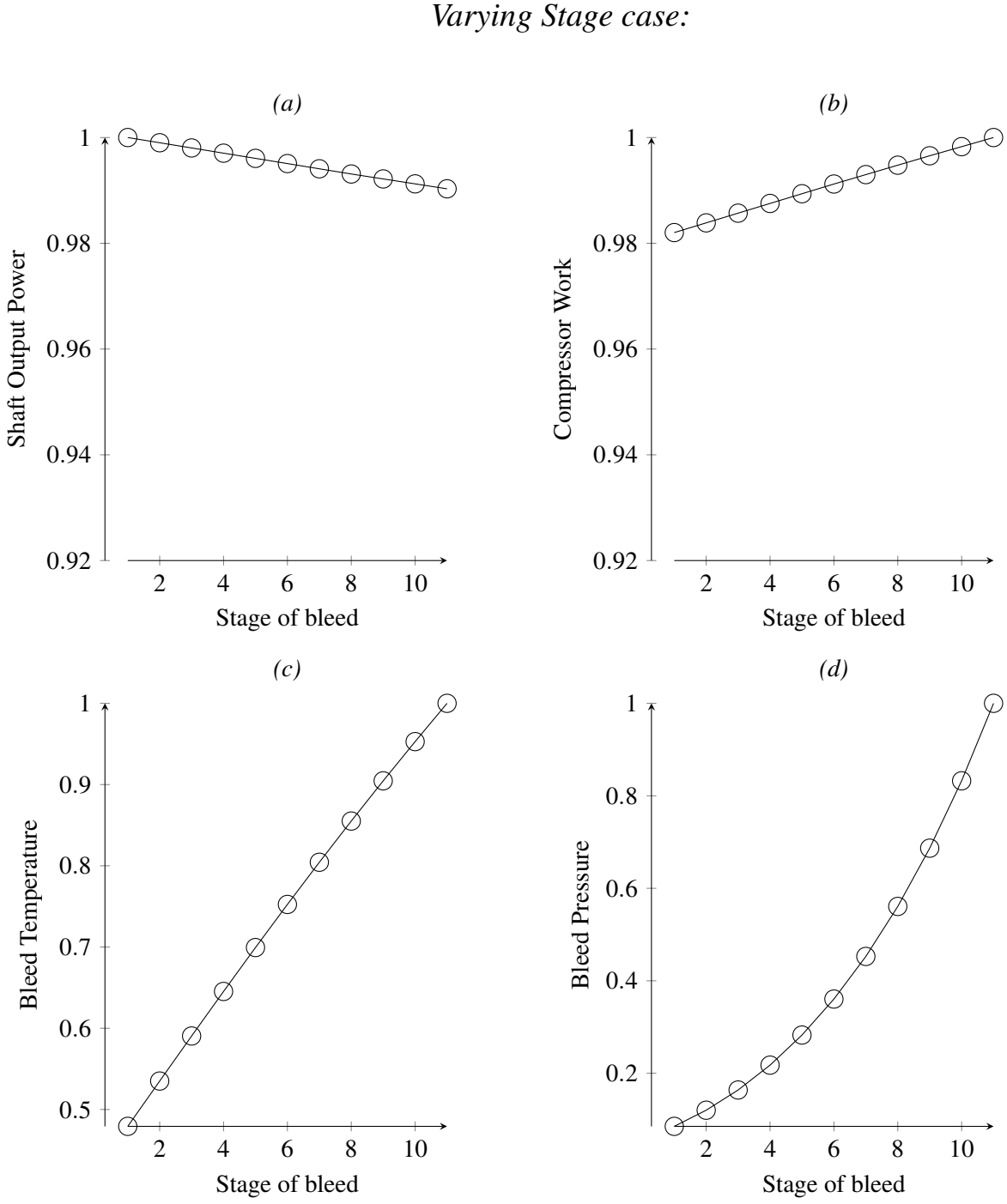

Figure 5.4: Results from varying stage case (from stages 0 to 11). Values are normalised to max value for each parameter.

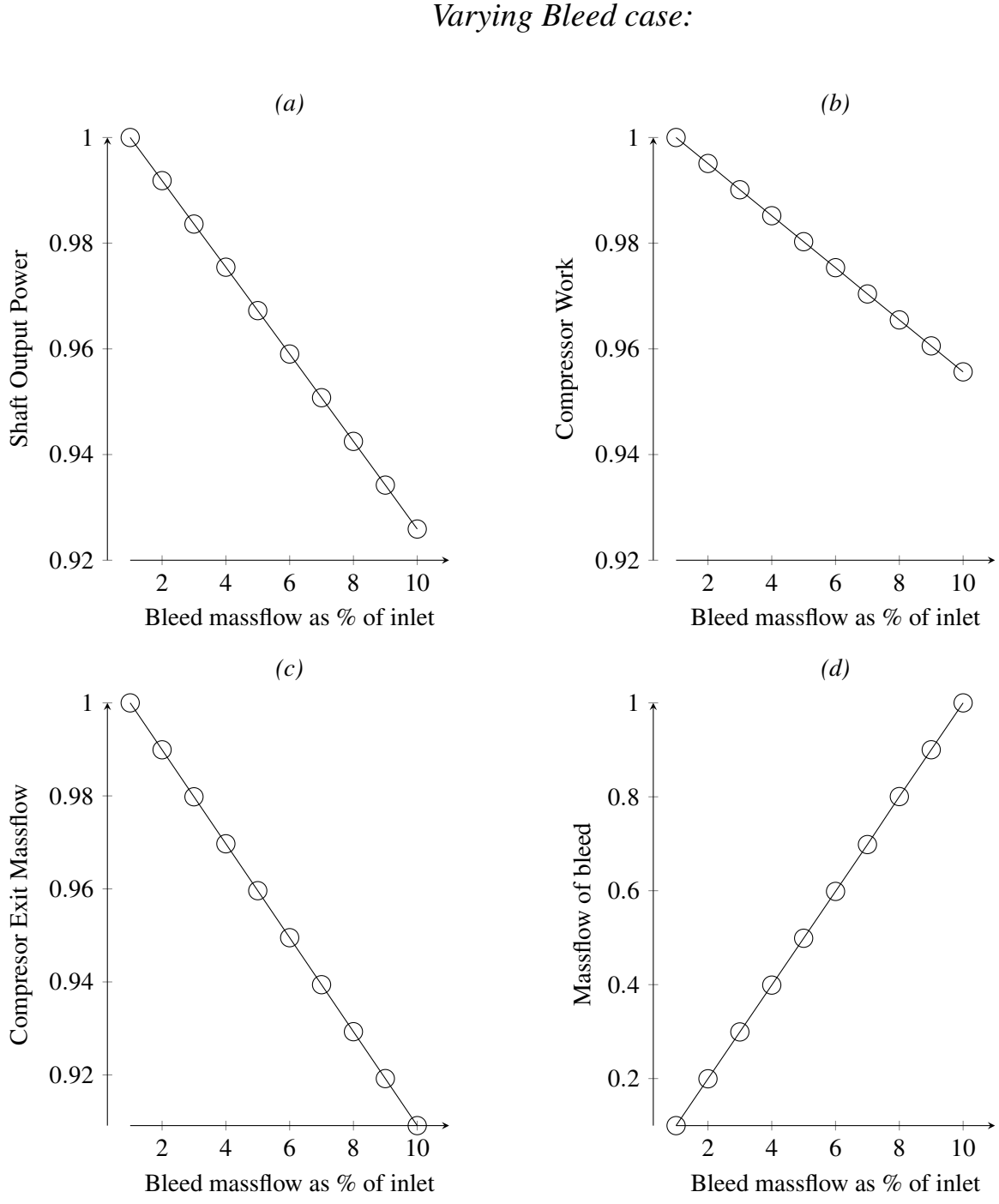

Figure 5.5: Results from varying bleed case (from 0% to 10%). Values are normalised to max value for each parameter.

5.4.2 Comparison to other methods

While chapter 4 shows that the method to derive stage pressure and temperature is sound, and section 5.4.1 shows the effect of bleed on gas turbine cycle using the new method, nether verify the accuracy of using this method, nor offer a comparison to other methods. Therefore a comparison at design conditions with **varying bleed flow** has been made against two other methods previously discussed in section 2.5.4:

1. **"All bleed at compressor exit"**. This method uses the assumption of all bleed is at the compressor exit. The user simply assumes that all interstage bleed occurs at the compressor exit, prior to combustion. No assumptions of bleed temperature and pressure are required, but conversely this means that these values will be highly inaccurate when downstream remixing is introduced (this may or may not be an issue depending on what the bleed air is used for). While this method does ensure that the bleed air is not part of the main gas path into the combustor, it makes no assumption of the change in work requirements for the compressor.

2. **"Splitting of the compressor"**. Splitting the compressor divides the compressor into a number of sub-compressors according to the location of the interstage bleed(s), as shown in figure 5.6. The operator must then determine the design point temperature and pressure for each sub-compressor, as well as selecting a relevant non-dimensional map for each sub-compressor. Design point polytropic efficiency must also be used over isentropic efficiency, as isentropic efficiency is highly stage-count dependent. If accurate sub-compressor design point conditions are selected then this method can yield accurate results, but it requires significant manual adjustments, and a very careful selection of the compressor maps used for each section.

3. **"New integrated method"**. This method represents the theories proposed within this report. It offers the improved accuracy of the 'split' method without the need for the associated manual calculations and assumptions (and resulting potential for human error in the manual calculations). Furthermore, it uses the polytropic efficiency derived pressure ratio.

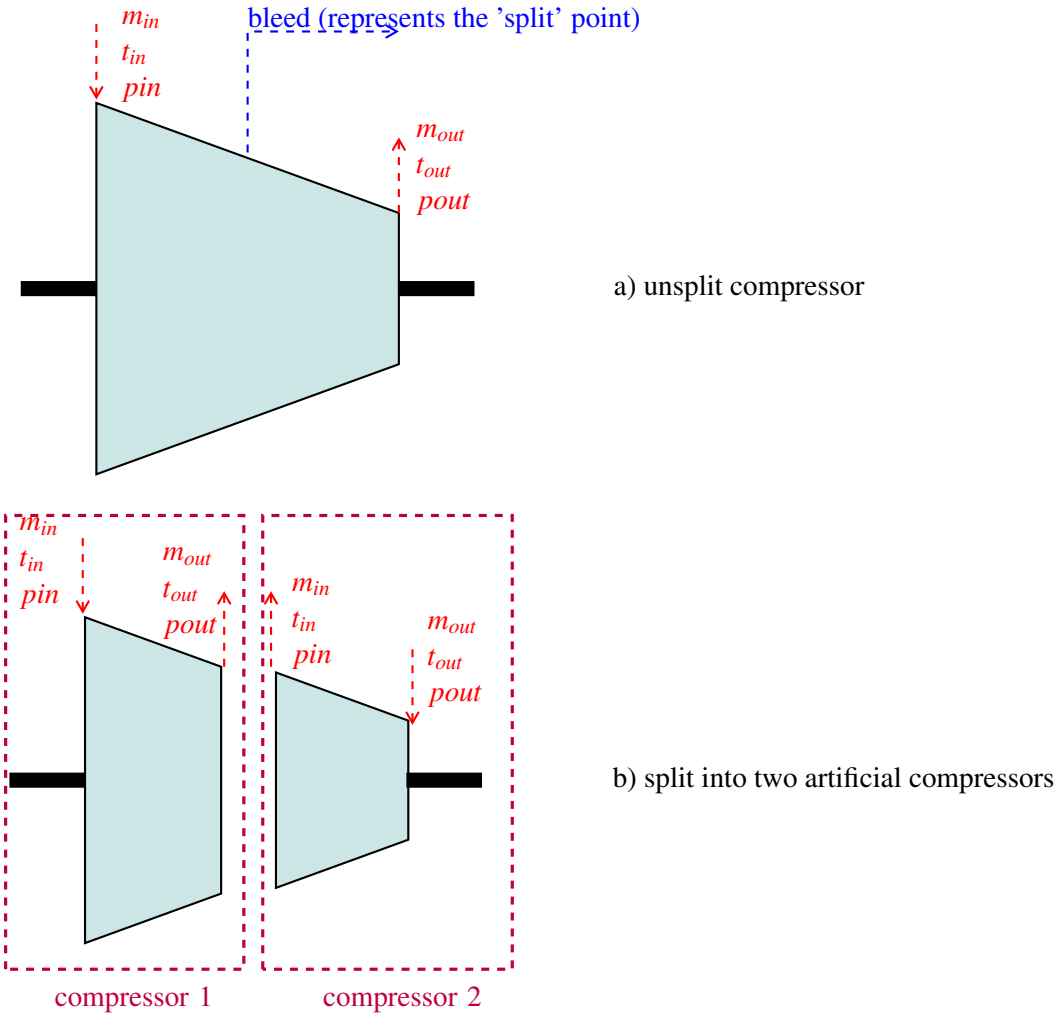

Figure 5.6: Splitting of the compressor

5.5 Analysis

Each of the three methods have been compared in *Turbomatch*. Figure 5.7 shows the effect of varying the amount of interstage bleed. In terms of shaft output power *(a)*, both the" new integrated method" and "splitting" method remain within $\pm$ 0.2% of each other. The 'all bleed at compressor exit" method, however, deviates by as much as 5% from the other two methods. This is a trend reflected in the fuel flow plot *(d)*. Compressor work *(b)* shows a slightly poorer agreement between the integrated and split methods (approximately 0.7%), and this is probably due to the use of two sub-compressors in the "split" case, compared to one in the integrated method. Finally, exhaust temperature demonstrates agreement within 10 degrees K (1%) between the split and integrated method, suggesting that the overall cycle is being calculated in similar ways for both cases.

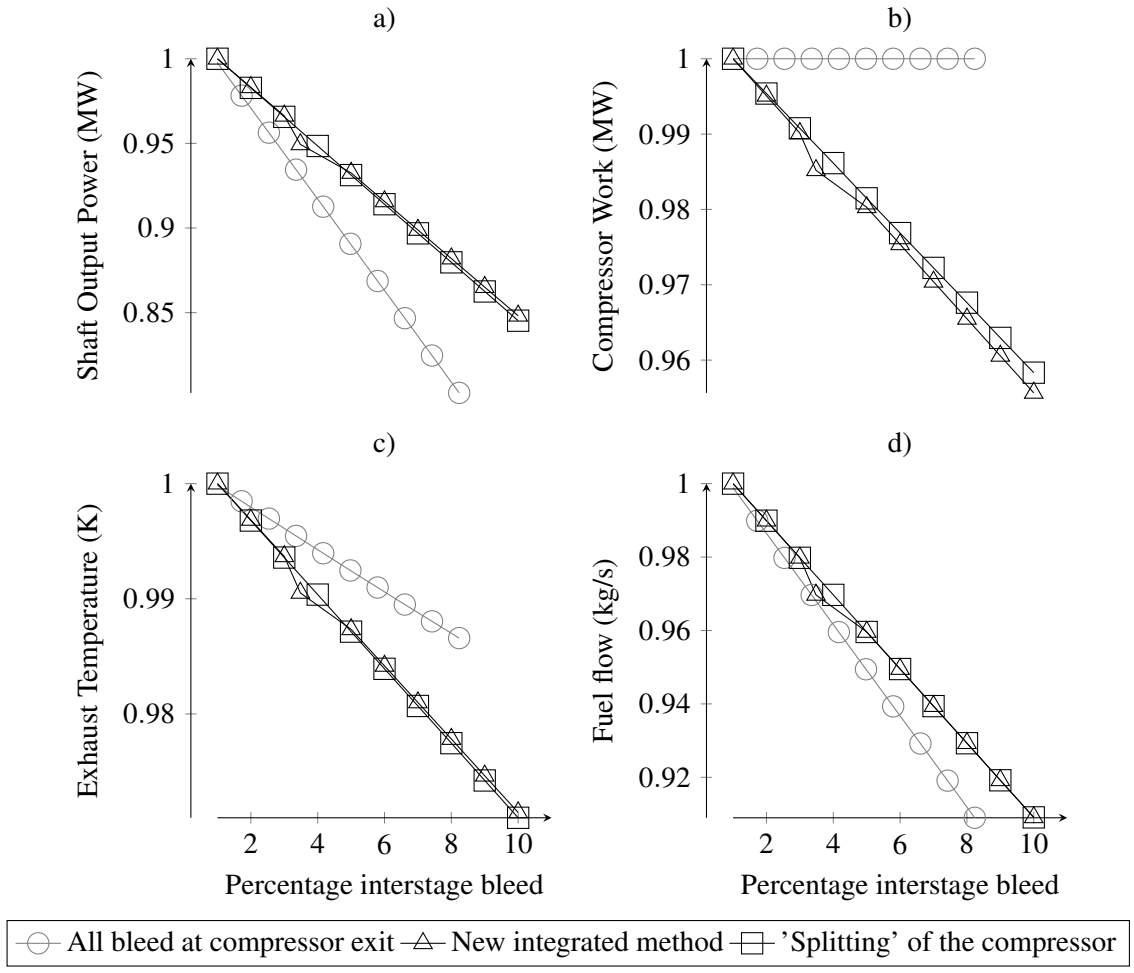

Figure 5.7: Effect of modifying bleed from 2% to 10% at design point.

Overall it can observed that the method 1 (all bleed at compressor exit) is significantly different to the other two cases. This suggests that its use as a modelling assumption is limited. Methods 2 and 3 ('splitting' of the compressor and new integrated method) show good agreement with each other, which is encouraging as it suggests that the thermodynamic properties using either method are similar, even though a different method has been used to derive each set of data. Bleed stage temperature and pressure for these methods has been derived using the same method described in chapter 4 (i.e. using linear temperature rise and polytropic derived pressure rise).

Off-design comparison

Analysis so far has been performed at design conditions. Discarding the method of assuming all bleed is at the compressor exit (as this had a relatively poor agreement with the other two methods),

the two remaining methods have been run over the same engine running line and compared to the same test data used in section 3.3. Shown in figure 5.8, it can be observed that at design point the two methods agree with the test data (as discussed above), but as load is reduced, the ”split” method data deviates significantly from the test data, while the new integrated method is relatively consistent with the test data along the whole working line. This is summarised in table 5.3 and discussed below.

Condition	**Output Power**		**Fuel Flow**		**Air mass flow**		**Pressure Ratio**	
	Split	*Alt.*	*Split*	*Alt.*	*Split*	*Alt.*	*Split*	*Alt.*
DP	1.4%	0.8%	0.8%	0.8%	0.0%	0.0%	1.2%	0.0%
OD1	1.7%	0.7%	1.9%	1.7%	0.3%	0.0%	1.7%	0.0%
OD2	2.1%	1.0%	2.1%	1.8%	0.5%	0.2%	2.1%	0.3%
OD3	3.5%	0.6%	2.2%	1.3%	1.7%	0.0%	6.6%	0.6%
OD4	17.8%	4.4%	6.5%	3.6%	7.1%	-0.3%	23.1%	1.5%

Table 5.3: Comparison of methods using test data (*Split*=”splittiing” of the compressor, *Alt.* = new alternative method).

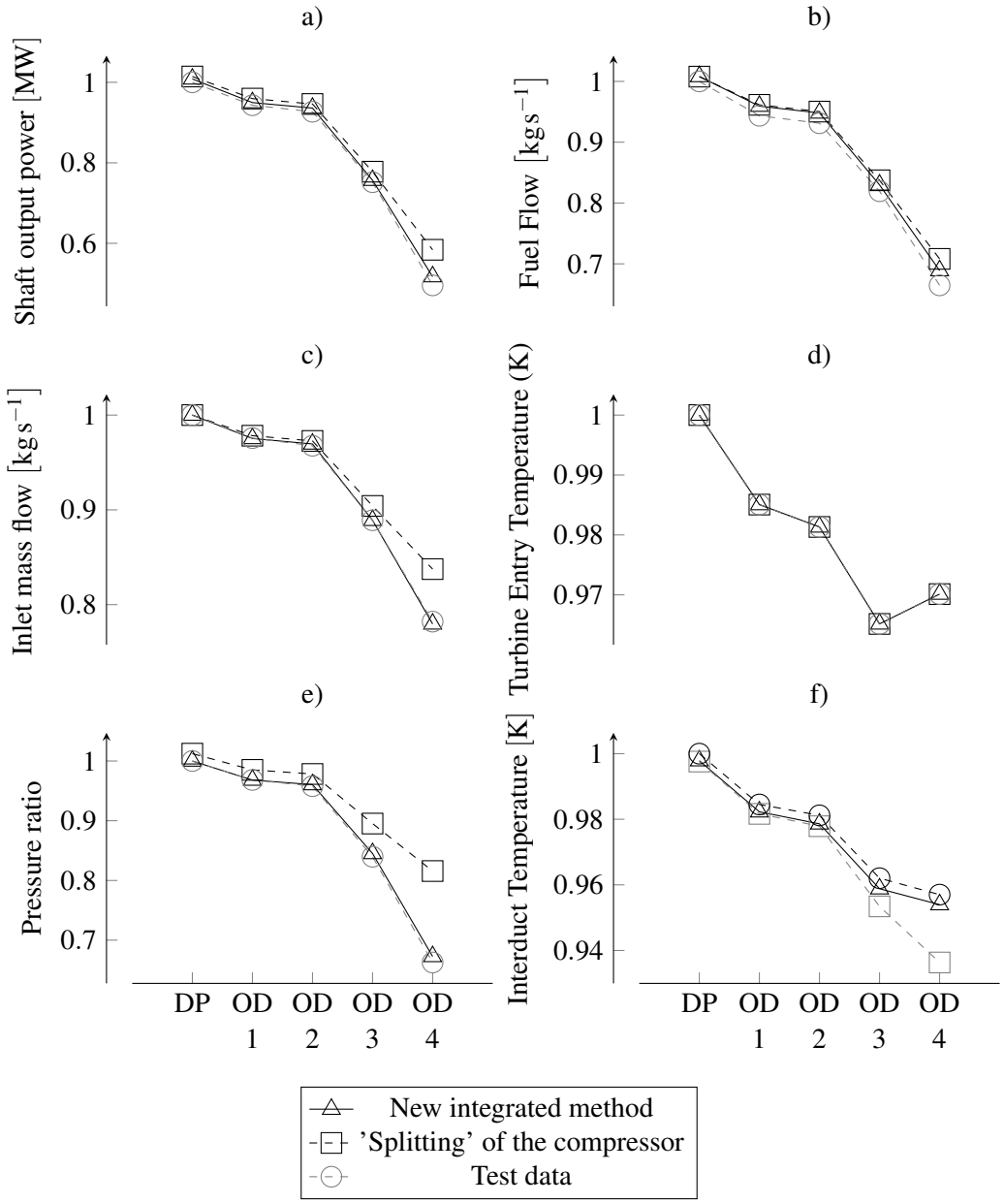

DP= Design Point
OD1 = TET= $(designpoint - 24K)$, No turndown air (97% load)
OD2 = TET= $(designpoint - 30K)$, No turndown air (93% load)
OD3 = TET = $(designpoint - 56K)$, 3.1% turndown air (75% load)
OD4 = TET= $(designpoint - 48K)$, 11.5% turndown air (48% load)

Figure 5.8: TurboMatch vs. Test data for selected output parameters

Alternative Method

For all parameters aside from fuel flow, the alternative method is within $\pm$ 1% of test data for the design point and all but the final off-design point. Fuel flow is typically within 1.5% of test values for all but the final off-design point. For all parameters, the fourth off-design conditions shows a weaker agreement, with 4% difference in power, 4% in fuel flow, and 1.5% difference in pressure ratio. Air mass flow, however, remains within 0.5% for all conditions.

The final off-design condition represents a low-load condition with a significant amount of turn-down air. The amount of turndown air is calculated based on the assumption that off-design non–dimensional turbine flow capacity will not deviate significantly from the design point value, and thus by iteration of test data through the adjustment of inlet mass flow until a non-dimensional turbine flow capacity equivalent to the design point value is achieved, turndown air may be calculated. This itself may introduce some errors and uncertainties into the test data calculations. This condition also represents the furthest point from design conditions, and thus any inaccuracies in the (generic) compressor map will be the largest here.

Considering the various test data measurement and calculation uncertainties, and uncertainties in the model due to the assumptions used and generic scaled maps, the alternative method models test data in a satisfactory manner (of course, final accuracy requirements will depend on the task in hand).

Split Method

The split method shows similar agreement with the alternative method for the design-point and the first off-design condition. However, agreement with test data reduces for subsequent off-design conditions. The difference in output power is over 3% at OD3, and more than 17% at OD4. Similar trends can be seen for the fuel flow and pressure ratio differences.

It is likely that the choice of compressor map and scaling method used in the split case is having a significant effect on accuracy at off-design conditions. Maps are chosen within Turbomatch based on the design point pressure ratio. If a map is selected based on a pressure ratio significantly different from the design point, then errors due to map scaling may become significant. In the case of the split compressor exercise, the first sub-compressor in particular is likely to be affect by this.

This can be solved by carefully selecting the relevant maps, or designing a custom map, but this in itself shows the benefit of using the alternative method - there is much less manual adjustment required over the split method.

Comparison to initial Turbomatch validation exercise Comparing the design-point results in table 5.3 to the initial model exercise done at design point only (table 3.4) shows generally consistent agreement. Output power difference is 0.5% in the initial model exercise, compared to 0.8% using the 'alternative' method. Air mass flow shows zero difference when compared to test data for both models. More interestingly, fuel flow difference is greater in the initial model (-3.2%), and is much improved (-0.8%) in the alternative model. This may indicate that the bleed assumptions in the initial model (placing all bleed at the compressor exit) are too simplistic for the thermodynamic calculation of fuel flow.

Chapter 6

Discussion

The following theories were investigated:

1. The further along the compressor the bleed is, the less 'benefit" from not having to do work on it, and conversely, the more bleed at bleed stage n, the greater the reduction in compressor work required
2. Bleed will always result in net loss of shaft output power, and increasing the amount of bleed will have greater negative effect than increasing the bleed stage
3. Assuming equal temperature rise and polytropic efficiency for all stages, stage pressure can be calculated for modern compressors and used in bleed calculations

These theories have been demonstrated through a number of calculation methods and by comparison to test data.

6.1 Method of estimating bleed stage pressure, temperature and work

Based on a study of a number of Siemens engines of varying technological levels, it was observed that stage-by-stage temperature rise within an axial compressor can be assumed to be linear. Analysis showed that stage temperature rise is within 0.9 ± 0.1 of normalised temperature rise. Older engine technology tended to have less of a linear rise (variation was 0.8 ± 0.2 of normalised temperature rise), but still sufficiently linear that it can be used for first approximations in 0-D modelling software.

Stage polytropic efficiency was also also observed to be linear and varied very little between stages (0.95 ± 0.05). While older technology engines tended to show a reduction at the front and

back stages (probably due to higher loading on these stages), the general trend showed broadly consistent polytropic efficiency between stages.

Hence, using an assumption of linear temperature rise and polytropic efficiency, and applying the polytropic relationship between pressure and temperature, an estimation of stage-by-stage compressor characteristics can be made. It has been shown in figure 4.3 that this method achieves results within 3% of the baseline cases (which represent different technological development levels). While it is outside the scope of this study to define the maximum acceptable error, it is shown that this method produces much more accurate predictions of pressure than a simple linear pressure rise calculation (as is currently used in some modelling software). Ultimately, an assessment of the accuracy will be made depending on the required use of the data and precision requirements.

It should be noted, however, that while a number of different engines with different technology levels were used in this study, they are all from the same manufacturer. It would be beneficial to conduct a similar exercise on an engine from a different manufacturer.

6.2 Effect of bleed on engine cycle

The effect of bleed on engine cycle was investigated in two ways. Firstly, by varying bleed stage between 1 and 11, but using the same amount of bleed each time ("*varying stage case*"). Secondly, by varying bleed amount between 0 and 10% at a fixed stage ("*varying bleed case*"). According to the theory presented in section 5, both should result in net loss of shaft output power, although varying the amount of bleed flow should be more detrimental than varying stage.

For both cases, shaft output power is reduced compared to the no-bleed case. However, the power loss is clearly greater in the varying bleed case (8%) than the varying stage case (1%) despite the fact that there is a net reduction in compressor work of 4% in the varying bleed case but a net *increase* of compressor work by 2% in the varying stage case. This is because the more flow that is used as bleed, less flow is available in the combustor. Hence for a given temperature, the lower the fuel input and hence the lower the net heat input. This has a more detrimental effect on net output power than varying the bleed stage.

Both cases show that shaft output power is reduced compared to a no-bleed case, and that the power loss is greater in the varying bleed case. Overall, the results are consistent with the theories stated in section 5. It has been shown that bleed affects compressor work requirements and the mass flow through the combustor, and due to both of these factors, ultimately affects the gas turbine cycle, output power and efficiency.

6.3 Comparison of new method to current methods and test data

After discarding the method of assuming all bleed is at the compressor exit (figure 5.7) due to the relative inaccuracies observed, the new integrated method and the 'split' compressor methods were compared to test data. Results show that at design condition both methods were broadly in agreement with test data, but as the engine moves away from design point, the 'splitting' method deviates significantly from the test data.

Using the alternative method, the difference between test data and the model is within $\pm$ 1% of test data for the all but the final off-design condition. For all parameters, the fourth off-design conditions shows a weaker agreement, with 4% difference in power, 4% in fuel flow, and 1.5% difference in pressure ratio. Air mass flow, however remains within 0.5% for all conditions

Considering the various test data measurement and calculation uncertainties, and uncertainties in the model due to the assumptions used and generic scaled maps, the alternative method models test data in a satisfactory manner without the need for extensive manual adjustment required in other methods (such as the split compressor method).

The split method initially shows similar agreement with the alternative method for the design-point and the first off-design condition. However, agreement with test data becomes worse for subsequent off-design conditions. The difference in output power is over 3% at OD3, and more than 17% at OD4. Similar trends can be seen for the fuel flow and pressure ratio differences. It is likely that the choice of compressor map and scaling method used in the split case is having a significant effect on accuracy at off-design conditions. If a map is selected based on a pressure ratio significantly different from the design point, then errors due to map scaling may become significant. This can be solved by carefully selecting the relevant maps, or designing a custom

map, but this in itself shows the benefit of using the alternative method - there is much less manual adjustment required over the split method.

While the split method deviated significantly from test data at low load off-design conditions, the integrated method demonstrated satisfactory agreement with the test data across the operating range of the engine. This suggests that this method offers a viable alternative to other modelling methods, whilst not increasing the complexity of the modelling tools.

6.4 Analysis of effect on compressor running line

The effect of bleed on the running line of the compressor may be investigated using the modelling software and test data. Figure 6.1 shows the running line with changing amount of bleed from 2% to 10%, whilst figure 6.2 shows the running line with changing bleed stage from stages 2 to 10, but at a constant bleed flow of 5%. Note that all running lines are analysed at the same turbine entry temperature for each respective test point (in other words, turbine entry temperature is the fixed parameter, or engine 'handle'). Also shown on these plots are the surge characterisics of the data points. The surge characteristic, Z, is a measure of how close the data point is to the pressure ratio at which surge will occur. It is expressed as a ratio of current data point to surge line:

$$Z = \frac{\Pi - \Pi_{choke}}{(\Pi_{surge} - \Pi choke)} \tag{6.1}$$

Where Π = compressor ratio. Thus the higher the value of Z , the less margin there is to surge. This term is often called the *surge margin*.

For increasing bleed (figure 6.1), it can be seen that the running line moves *down* relative to to the nominal case. It is shown that for a given inlet air mass flow, pressure ratio is reduced. As more air is bled from the compressor, there is less air available for combustion, and hence for the same firing temperature there will be less energy available for expansion through the turbine. This means that the turbine does not extract as much energy from the gas path as previous, and hence the compressor is not required to deliver such a high pressure ratio (compressor speed will hence reduce). However, the effect of this 'rematching' between the compressor and turbine results in

an *increased* surge margin for a given load, which is consistent across the running line. Put very simply this suggests that for a given mass flow, increasing bleed at a specified stage improves surge margin but at the cost of cycle efficiency.

It can be seen that increasing the bleed stage, but keeping the amount of bleed fixed (figure 6.2) has the effect of moving the running line to the left. For a given non-dimensional mass flow, increasing the stage has the effect of reducing surge margin at low running conditions, but having less effect near design point conditions. It is likely that the loss in cycle efficency means the turbine and compressor match at a lower pressure ratio, and hence the running line is moved to the left.

Air mass flow is constant in this case, so there is no penalty though the combustion process. Instead, bleeding at later stages does unnecessary work on the bleed air (unnecessary form the point of view of the engine cycle - not necessarily secondary air requirements!) that effectively increases work requirements in the compressor. Increasing the compressor work requirements reduces the useful work available to the cycle, and hence reduces output power.

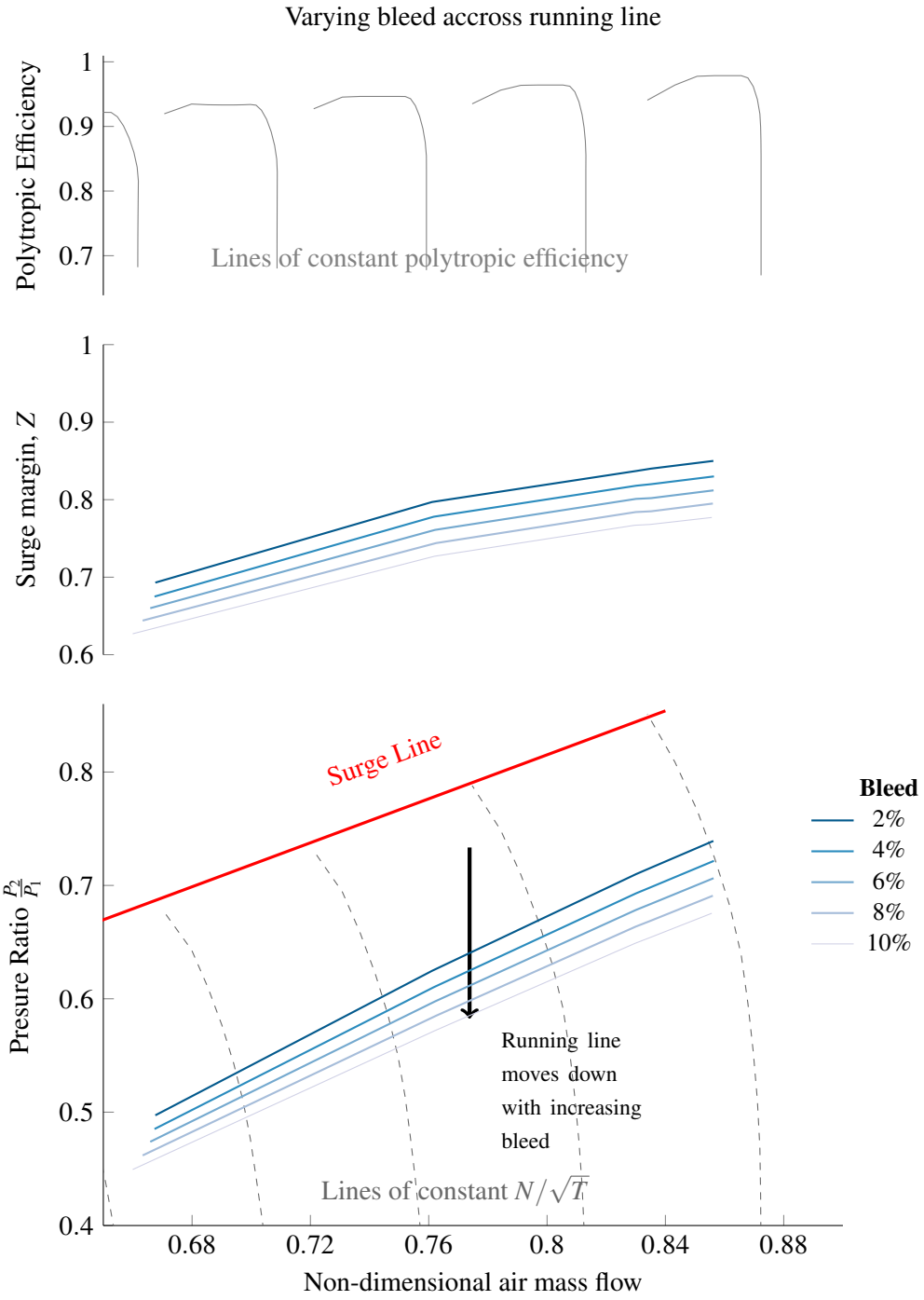

Figure 6.1: Compressor Map for varying bleed amount at stage 9 (values are normalised)

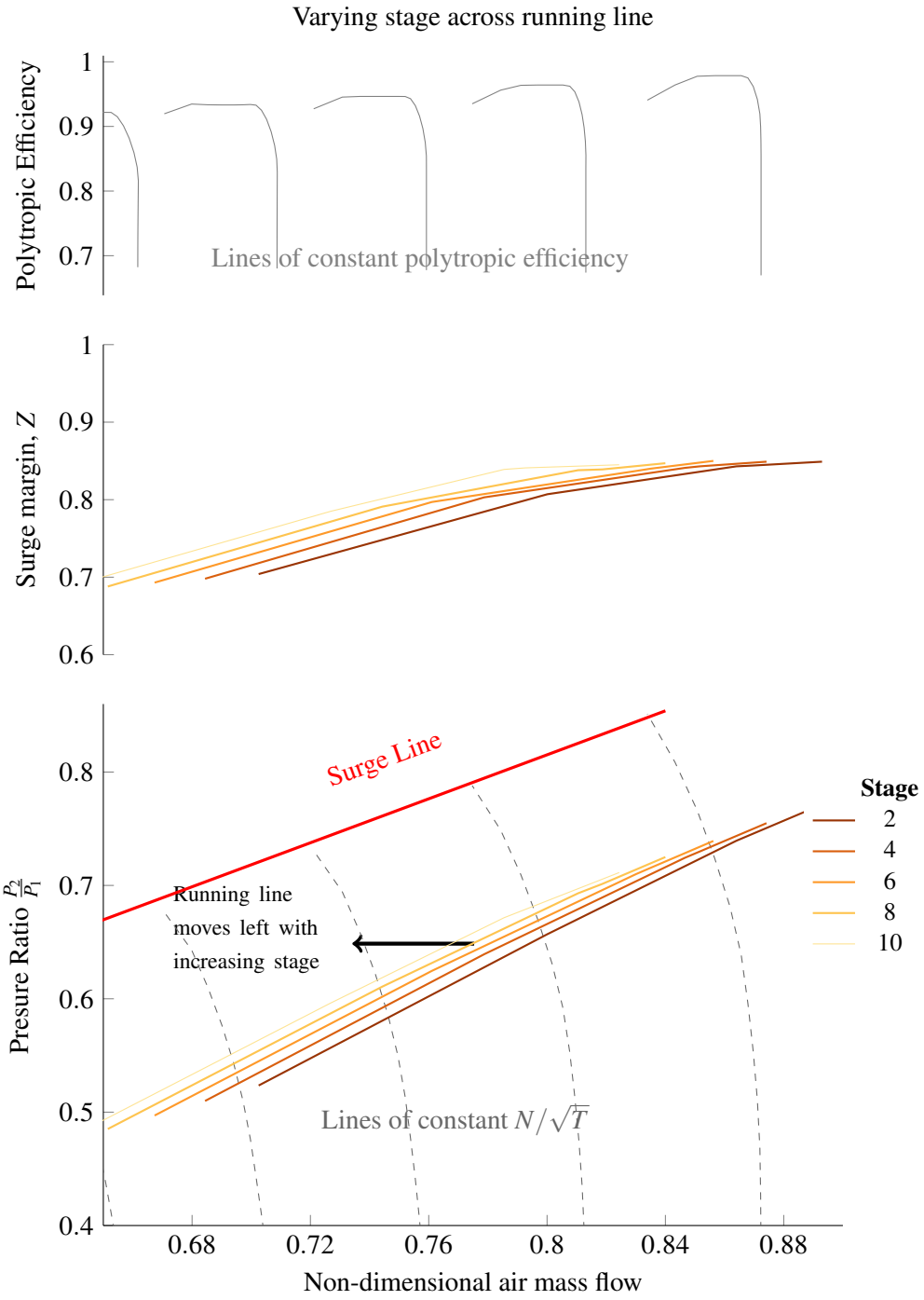

Figure 6.2: Compressor Map for varying stage using fixed bleed of 5% (values are normalised)

Both plots demonstrate that the compressor running line is changed with bleed, but the compressor does not act in isolation, and the entire gas turbine cycle is affected. Clearly, one cannot look at bleed amount and stage in isolation. To further investigate, the relationship between these two parameters requires analysis together. Contour plots showing surge margin and thermal efficiency using varying bleed and stage as independent variables have been produced (figure 6.3). In these plots, turbine entry temperature is constant. These show that the optimum location for maximum surge margin at fixed turbine entry temperature is at high stage/high bleed, but this is also the point where the greatest cycle efficiency loss is seen, and losses are likely unacceptable. In the example shown, the plots are presented at fixed turbine entry temperature - probably not relevant for surge margin investigations where margin at a given speed is more useful. However, these plots do show how this method can be used to help the user identify the optimum location for bleed for a given stage or bleed amount.

By re-plotting at fixed speed or power, the user could produce plots suited to the particular issue they are investigating. For example, for surge margin investigations, fixed speed plots are likely most useful. When surge is not an issue (due to sufficient margin), the user is most likely interested in the effect of bleed for a given load on cycle efficiency.

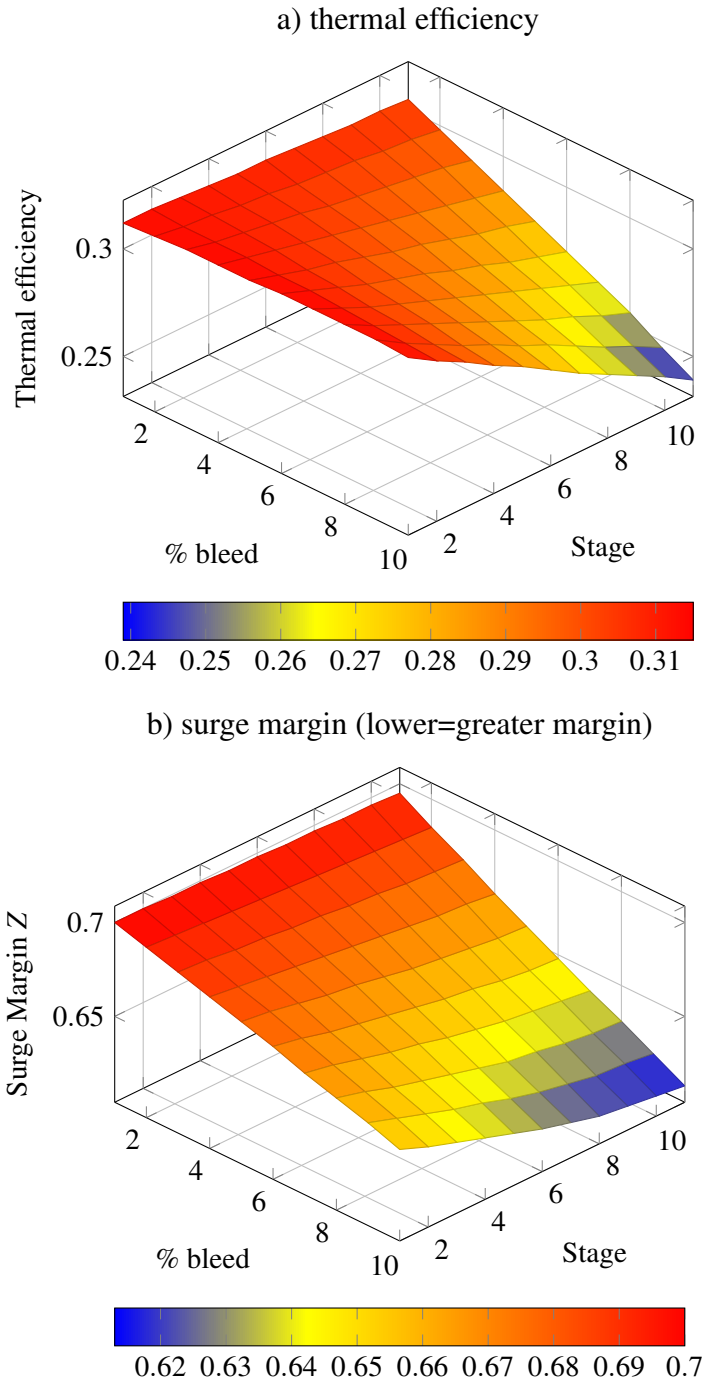

Figure 6.3: 3D contour plot of thermal efficiency and surge margin with varying bleed and stage

Chapter 7

Conclusion and Recommendations

7.1 Conclusion

By developing a method which offers an alternative method of simulating interstage bleed within a compressor without the need to compromise on model accuracy, the following has been demonstrated:

- The Cranfield 0-D modelling software "Turbomatch" has been validated against test data for a small industrial gas turbine, and it has been shown that it can model engine performance within 0.5% to 1.0% accuracy for most parameters - well within the measurement uncertainty of the test data. Fuel flow (b) is a little less accurate (around 3%), which is likely due to the different calculation methods between the test data and Turbomatch calculations, as well as over-simplistic bleed assumptions in the compressor. Fuel flow from the test data has been measured using a coriolis massflow meter, which will have an associated uncertainty of up to 1%. The Turbomatch data, however, calculates fuel flow based on the thermodynamic (calculated) heat input into the engine and a generic fuel calorific value.

- By using the isentropic expression for pressure and temperature, and assuming overall compressor polytropic efficiency represents stage efficiency, and that stage temperature rise is linear, it has been demonstrated that stage pressure rise can be calculated within 3% for a number of different engines of varying technology. This was shown using case studies from a number of Siemens industrial gas turbines

- Compressor and gas turbine cycle changes due to bleed can be calculated according to the "superposition principle" (i.e. the assumption that the work done on bleed air m at stage n, plus the work that *would have been done* had the flow remained part of the gas path, is equal

to the work done by the same amount of massflow without any bleed offtake). This method has been implemented in the Cranfield modelling software *Turbomatch*, which itself has been validated against test data from an industrial engine. Analysis so far show the method is quick, accurate, and compares well to test data.

- This method, called the ”alternative method”, has been shown to be quicker and more accurate when compared to other methods, such as compressor ’splitting’, especially at off-design conditions.

- By using the method to vary bleed stage and amount, it has been shown that changes to the engine running line, and hence surge margin, can be made by changing the bleed offtake parameters. This also has an effect on overall cycle efficiency. This method can be used to produce three-dimensional plots showing the combined effects of beed amount and offtake location at a range of fixed parameters according to the user requirements (e.g. fixed speed, temperature or massflow)

The alternative method has been shown to allow for the simulation of interstage bleed in a gas turbine compressor without the need for complex modelling or artificial ’splitting’ of components. Comparison of this method against a compressor ’splitting’ methods showed comparable results can be obtained with the need for extensive manual model adjustment that the splitting method requires.

While it is difficult to quantify whether the accuracies are ’acceptable’, as accuracy requirements vary considerably depending on the task in hand, it must be appreciated that this method has been implemented in 0-D cycle analysis software, which uses thermodynamic principles and component maps to calculate engine performance. Such a model tends to be used to analyse the overall effects of a component change on the engine cycle in a rapid and low-complexity manner (at a range of off-design conditions), whilst still producing a satisfactory level of accuracy. More detailed analysis is done by other tools, such as CFD, but in the initial stages of a design project, the quick analysis and results from the 0-D software are essential to narrow down design choices and to analyse off-design performance. In this respect, the alternative method offers an enhancement to current methods for modelling bleed in the gas turbine.

7.2 Recommendations

It is recommended that the results from the 0-D simulation tool are compared to results from another modelling tools, such as CFD or stage-stacking methods.

Furthermore, it would beneficial to assess the accuracy of this method using custom compressor maps specific to the engine modelled. It is also recommended that the method is performed on a number of different engines of varying technology levels and pressure ratios. As this study focussed on an industrial engine, it would be useful to compare results using an aero-engine.

Appendix A

Sample Calculation - pressure derivation

The following example demonstrates the calculation of stage-by-stage pressure rise using the method described in section 4. A generic example of an industrial gas turbine is used for this sample calculation. Typical design point compressor conditions are shown in table A.1.

A.1 Calculate stage pressure rise

From equation 4.1, stage temperature rise (ζ) is linear, based on the number of compressor blade stages:

$$\zeta = (T_3 - T_2)/n_{last}$$
$$\zeta = \frac{(707.4 - 288.15)}{11} = 38.13K$$

Parameter	**Details**
Compressor pressure ratio	17.8:1
Compresor stages	11
Inlet Temperature	288.15K
Inlet Pressure	1.013bar
Compressor exit temperature	707.4K
Compressor inlet air flow	38.9kg/s

Table A.1: Parameters for sample calculation

A.2 Calculate overall polytropic efficiency from overall isentropic efficiency

Assumption: Gamma is based on average temperature in compressor for dry air

Polytropic efficiency (η_{poly}) may be directly stated, derived from isentropic efficiency, or calculated. As design point values are known in this example, the polytropic efficiency will be calculated

Pressure ratio (*PRC*) can be used to obtain compressor exit pressure:

$$\Pi = \frac{P_3}{P_2}$$
$$P_2 = \Pi \times P_1 = 17.8 \times 1.013 = 18.032$$

Using equation 2.12:

$$\eta_{poly} = \frac{\ln\left(\frac{P_3}{P_2}\right)^{\left(\frac{\gamma-1}{\gamma}\right)}}{\ln\left(\frac{T_3}{T_2}\right)}$$
$$\eta_{poly} = \frac{\ln\left(\frac{18.032}{1.013}\right)^{\left(\frac{1.3822-1}{1.3822}\right)}}{\ln\left(\frac{707.4}{288.15}\right)} = 0.8860$$

A.3 Calculate first stage pressure ratio

Assumption: Temperature rise is constant for all stages Assumption: Polytropic efficiency is constant for all stages Assumption: Cp and gamma based on dry air at the average of stage inlet and outlet

Knowledge of the polytropic efficiency allows calculation of stage pressure ratio. This is demonstrated below for one stage (stage 1), and results for the other stages are tabulated in table A.2.

Inlet temperature to stage 1 288.15K

Temperature rise stage 1	38.13K
Polytropic efficiency	0.8860
CP	1.004
Gamma	1.400

Pressure ratio for stage 1 using equation 4.4:

$$\pi_n = \left(\frac{T_{n-1}+\zeta}{T_{n-1}}\right)^{\eta_{poly}\left(\frac{\gamma}{\gamma-1}\right)}$$

$$\pi_1 = \left(\frac{288.15+38.13}{288.15}\right)^{0.8860\left(\frac{1.4}{1.4-1}\right)} = 1.47$$

Thus the pressure ratio, π, for stage 1 is 1.47, resulting in a stage exit pressure of $1.47 \times 1.013 = 1.489$bar. The *pressure factor* (ratio of stage pressure to overall pressure) is also calculated.

Results are shown graphically in figure A.1. It can be seen that the derived pressure matches well with the actual pressure. Now that each blade stage pressure and temperature are defined, it is relatively simple to obtain the bleed stage properties. For, example, for stage 6:

Temperature	516.8K
Pressure	6.307bar
CP	1.029

stage	**S1**	**S2**	**S3**	**S4**	**S5**	**S6**	**S7**	**S8**	**S9**	**S10**	**S11**
ζ	38.13	38.13	38.13	38.13	38.13	38.13	38.13	38.13	38.13	38.13	38.13
T_1, K	288.2	326.1	364.3	402.4	440.5	478.6	516.8	554.9	593.0	631.2	669.3
T_2, K	326.1	364.3	402.4	440.5	478.6	516.8	554.9	593.0	631.2	669.3	707.4
Average T, K	307.1	345.2	383.3	421.5	459.6	497.7	535.8	574.0	612.1	650.2	688.3
C_p	1.004	1.007	1.011	1.016	1.022	1.029	1.036	1.045	1.053	1.062	1.072
γ	1.400	1.399	1.397	1.394	1.391	1.387	1.383	1.379	1.375	1.370	1.366
π_{stage}	1.470	1.410	1.364	1.328	1.299	1.276	1.256	1.239	1.225	1.212	1.201
Pexit, bar	1.489	2.100	2.865	3.805	4.944	6.307	7.920	9.813	12.017	14.565	17.495
$P_f fact$	0.09	0.12	0.16	0.22	0.28	0.36	0.45	0.56	0.69	0.83	1.00

Table A.2: Estimation of stage characteristics, compressor

It is then relatively straightforward to calculate the enthalpy and work done on the bleed air, which can then be fed into the overall modelling cycle.

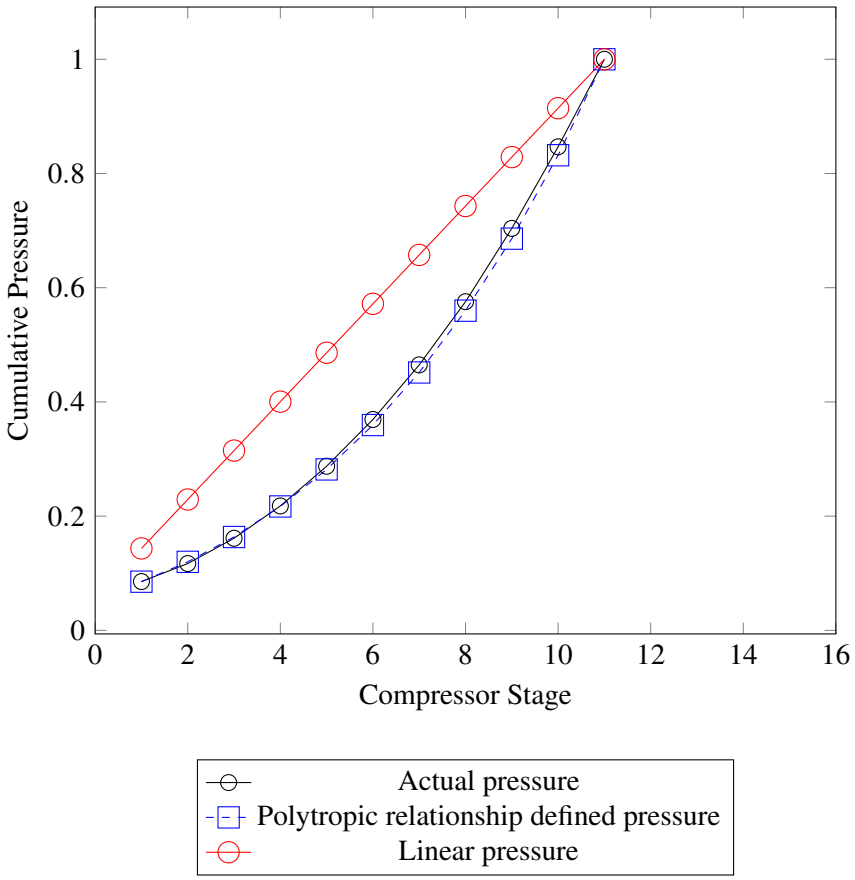

Figure A.1: Pressure rise per stage - SGT400

Appendix B

Assumption that overall polytropic = stage isentropic efficiency

The following example demonstrates the difference between stage pressure rise using the following:

1. The assumption that the stage polytropic efficiency is approximately the same for each stage, and that *overall* polytropic efficiency can be used as an assumption for *stage* polytropic efficiency
2. The assumption that stage *isentropic* efficiency can be estimated as being the same as overall *polytropic* efficiency, as the stage pressure ratios are small enough that there is little difference between isentropic and polytropic (see figure 2.7).

The method stated in number 1 has been discussed in detail in section 4.4.3 and appendix A. The method stated in number 2 is based along a similar method but uses the isentropic expression to define stage pressure rise.

From equation 2.9, isentropic efficiency (eta_{isen}) is defined as:

$$\eta_{isen} = T_2 \left[\frac{(\Pi_{comp})^{\frac{\gamma-1}{\gamma}} - 1}{T_3 - T_2} \right] \tag{B.1}$$

This may be rearranged in terms of pressure rise to:

$$\Pi_{comp} = P_2 \left[\left(\frac{\eta_{isen} \times \zeta}{T_2} + 1 \right)^{\frac{\gamma}{\gamma-1}} \right] \tag{B.2}$$

Where ζ = equal stage temperature rise.

Applying this equation to the method detailed in 4.4.3 for the SGT-400 and SGT-100E+ allows a comparison between the polytropic and isentropic methods, as shown in figure B.1. This shows that for these two engines, there is minimal difference between the two methods, although it should be noted that the typical stage pressure ratio is less than 1.5:1. Whether the isentropic method compares well for higher pressure ratio stages would be an interesting investigation.

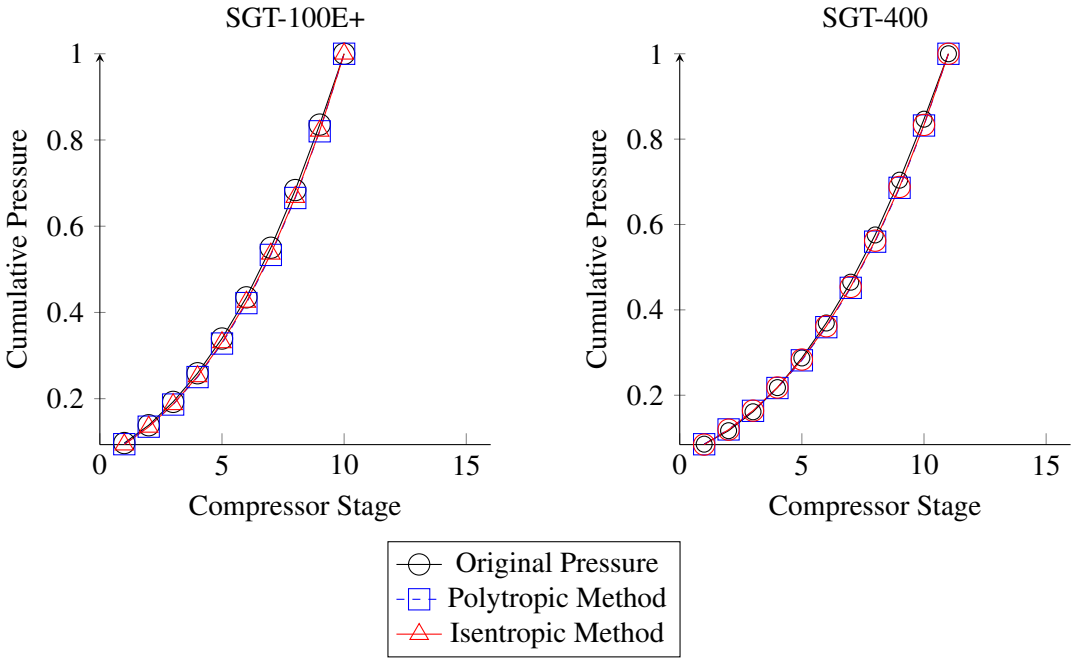

Figure B.1: Comparison between isentropic and polytropic method to derive stage pressure. Values are normalised to maximum pressure.

References

[1] Cohen H., Rogers GFC., S. H., 1996. *Gas turbine theory*. Pearson.

[2] Bolemant, M., and Peitsch, D., 2014. "An alternative compressor modeling method within gas turbine performance simulations". *Deutcher Luft- und Raumfahrtkongress*(340047), pp. 1–12.

[3] Cumpsty, N. A., 1989. *Compressor aerodynamics*. Longman.

[4] Siemens, 2018. SGT-400 Industrial Gas Turbine Technical Specifications. Accessed online on 29 March 2018 at https://www.energy.siemens.com/co/pool/hq/power-generation/gas-turbines/SGT-400/Brochure.

[5] SAE, 1974. Gas Turbine Engine Performance Station Identification and Nomenclature, Aerospace Recommended Practice, ARP 755A. Tech. rep., Society of Automotive Engineers, Warrandale, Pennsylvania.

[6] Miller, A., 2005. "Compressor Conceptual Design Optimization". Msc thesis, Georgia Institute of Technology.

[7] Follen, G., and AuBuchon, M., 2000. "Numerical Zooming Between a NPSS Engine System Simulation and a One-Dimensional High Compressor Analysis Code". *NASA Technical Memorandum; Computational Aerosciences Workshop 2000*, pp. 1–18.

[8] Alexiou, A., and Mathioudakis, K., 2009. "Secondary Air System Component Modeling for Engine Performance Simulations". *Journal of Engineering for Gas Turbines and Power,* **131**(3), may, p. 031202.

[9] Zhao, B., Shaobin, L., Qiushi, L., and Sheng, Z., 2011. "Numerical Research on Impact of Air System Bleedin G on Compressor Performance". In Transaction of Nanjiing University of Aeronautics & Astronautics, Vol. 1 of *AJK-Fluids2011*, ASME, p. 8.

[10] Walsh, P. P., and Fletcher, P., 2008. *Gas Turbine Performance*.

[11] BSI, 2010. *BS ISO 2314:2009 Gas turbines. Acceptance tests.* BSI Standards Limited.

[12] Foley, A., 2001. "On the Performance of Gas Turbine Secondary Air Systems". In Proceedings of ASME TURBO EXPO 2001, ASME.

[13] Wright, L. C., 1970. "Blade Selection for a Modern Axial-Flow Compressor". *Fluid Mechanics, Acoustic, and Design of Turbomachinery Part II,* **2**, pp. 603–626.

[14] Frost, G. R., Hearsey, R. M., and Wennerstrom, A. J., 1972. "A Computer Program for the Specification of Axial Compressor Airfoils". *ARL Report*(December), pp. 1–158.

[15] Jeschke, P., Kurzke, J., Schaber, R., and Riegler, C., 2004. "Preliminary Gas Turbine Design Using the Multidisciplinary Design System MOPEDS". *Journal of Engineering for Gas Turbines and Power,* **126**(2), p. 258.

[16] Song, T. W., Kim, T. S., Kim, J. H., and Ro, S. T., 2001. "Performance prediction of axial flow compressors using stage characteristics and simultaneous calculation of interstage parameters". *Proceedings of the Institution of Mechanical Engineers, Part A: Journal of Power and Energy,* **215**(1), pp. 89–98.

[17] Veres, J., 2009. "Axial and Centrifugal Compressor Mean Line Flow Analysis Method". In 47th AIAA Aerospace Sciences Meeting including The New Horizons Forum and Aerospace Exposition.

[18] Grimshaw, S. D., Pullan, G., and Hynes, T. P., 2016. "Modeling Nonuniform Bleed in Axial Compressors". *Journal of Turbomachinery,* **138**(9), sep, p. 091010.

[19] Bulat, D., 2012. *Preliminary Investigation Into the Integrated Approach of a Gas Turbine Design*. Cranfield University [MSc Thesis].

[20] Hamming, R., 1987. *Numerical Methods for scientists and engineers*, 2nd ed. Dover Publications.

[21] Smith, M. K. D., 1986. TRR 84/006 'PerfProg' (internal report). Tech. rep., Ruston Gas Turbines Ltd.

[22] Nikolaidis, T., 2015. *The Turbomatch Scheme*. Cranfield University [internal report].

[23] Alexiou, A., and Mathioudakis, K., 2005. "Development of gas turbine performance models using a generic simulation tool". In Proceedings of the ASME Turbo Expo, Vol. 1.

[24] GasTurb GmbH, 2017. *GasTurb 13. Design and Off-Design Performance of Gas Turbines*. GasTurb GmbH.

[25] European Council, 2010. "Directive 2010/75/EU Industrial Emissions". *Official Journal of the European Union,* **L334**, pp. 17–119.

[26] Grebenik, J., 2014. *TR 14/127*. Siemens [internal report].

[27] Bucker, D., Span, R., and Wagner, W., 2003. "Thermodynamic Property Models for Moist Air and Combustion Gases". *Journal of Engineering for Gas Turbines and Power,* **125**(1), p. 374.

[28] Kellner, T., 2016. GE Started Testing The World's Largest Jet Engine.